MONGOLIAN PHYSICAL SOCIETY

ISSN 2414-9756

MONGOLIAN JOURNAL OF PHYSICS

SUPPLEMENT 6, OCTOBER 2024

Published by Mongolian Physical Society

12th International Conference on Materials Science

(ICMS2024)

October 2-3, 2024

Abstracts

Edited by Dr. G. Erdene-Ochir[1], Dr. N. Tuvjargal[1], Acad. J. Davaasambuu[1, 2]

[1]*Department of Physics, National University of Mongolia*

[2]*Institute of Physics and Technology, Mongolian Academy of Sciences*

Ulaanbaatar

2024

DDC

015

X-71

Mongolian Journal of Physics. Supplement 6 presents the complete Abstracts of all contributions of the 12th International Conference on Materials Science (ICMS2024) in the National University of Mongolia and Institute of Physics and Technology, Mongolian Academy of Sciences, Ulaanbaatar, Mongolia, October 2-3, 2024.

ISBN 978-99973-55-42-3

Preface

Dear colleagues,

We are pleased to welcome you to the 12th International Conference on Materials Science (ICMS2024) which will be held at the National University of Mongolia and Mongolian Academy of Sciences from 2 to 3 October 2024 in Ulaanbaatar.

The objectives of the conference are to bring together scientists working in the field of materials science from around the world, to exchange ideas, recent research results in this area and to offer a platform for the initiation of scientific cooperation between Mongolian and foreign scientists.

The conference will focus on the structures, properties and applications of new materials as well as their characterization techniques.

We would like to express our gratitude to all sponsors for their support in the realization of this conference and to the authors for submitting their abstracts to the ICMS2024.

On behalf of the Scientific Committee

Acad. Jav Davaasambuu

CONFERENCE ORGANIZERS

Mongolian Physical Society, Mongolia

Institute of Physics and Technology, Mongolian Academy of Sciences, Mongolia

National University of Mongolia, Mongolia

Inner Mongolia Normal University, China

Institute of Physical Materials Science, Siberian Branch of the Russian Academy of Sciences, Russia

Buryat State University, Russia

CONFERENCE COMMITTEES

Scientific committee

- Acad. J. Davaasambuu (Mongolian Academy of Sciences, Mongolia)
- Prof. Ts. Baatarchuluun (Mongolian Physical Society, Mongolia)
- Prof. U. Pietsch (University of Siegen, Germany)
- Prof. B. Narsu (Inner Mongolia Normal University, China)
- Prof. O. Tegus (Inner Mongolia Normal University, China)
- Prof. A. Nomoev (Institute of Physical Material Science SB RAS, Russia)
- Acad. J. Temuujin (CITI University, Mongolia)
- Acad. O. Penyazkov (A.V.Lykov Institute, Belarus)
- Prof. S.P. Bardakhanov (Khristianovich Institute of Theoretical and Applied Mechanics of SB RAS)
- Prof. Altan Bolag (Inner Mongolia Nornal University, China)
- Acad. V.A. Orlovich (Institute of physics of NAS of Belarus, Belarus)
- Prof. E.M. Shpilevsky (Institute of physics of NAS of Belarus, Belarus)

Organizing committee:

- Dr. N. Tuvjargal (National University of Mongolia, Mongolia)
- Dr. G. Erdene-Ochir (National University of Mongolia, Mongolia)
- Dr. S. Munkhtsetseg (National University of Mongolia, Mongolia)
- Dr. G. Munkhbayar (National University of Mongolia, Mongolia)
- Dr. Tsetsenbaatar (Inner Mongolia Nornal University, China)
- E.Ch. Khartaeva (Laboratory of Composite Materials Physics, Institute of Physical Material Science of the Siberian Branch of the Russian Academy of Sciences, Russia)
- Dr. B. Otgongerel (Institute of Physics and Technoloy, MAS, Mongolia)

Scientific Program

02 October, 2024

(Conference Hall, Mongolian Academy of Sciences)

13.00-14.00	**Registration**
14.00-14.30	Opening Ceremony **Prof. Ts. Baatarchuluun,** *President of Mongolian Physical Society, Mongolia* **Acad. J. Davaasambuu,** *Director of Institute of Physics and Technology, MAS, Mongolia* **Prof. Dr. Andrey Nomoev,** *Director of Institute of Physical Material Science SB RAS, Russia* **Prof. Dr. Bai Narsu,** *Inner Mongolia Normal University, China*
Chairperson: Academician J.Davaasambuu	
14.30-15.00	**Invited talk by Academician. J. Temuujin** *CITI University, Mongolia* Characterization of low- and high-calcium pond ashes and their applicability for the preparation of alkali-activated pastes
15.00-15.30	**Invited talk by Prof. O. Tegus** *Inner Mongolia Normal University, China* Recent development of magnetic caloric materials
15.30-16.00	**Invited talk by Prof. O. B. Wright** *Hokkaido University, Sapporo, Japan* Maze balls and metabeams: how to stop sound in its tracks
15.45-16.00	Possibility of Detection of Hepatitis D Virus Using Surface Plasmon Resonance **G.Batzul** *Institute of Physics and Technology, Mongolian Academy 0f Sciences, Mongolia*
16.00-16.15	Surface properties of the mechanical exfoliated MoS_2 few layers **B.Odontuya** *Department of Physics, School of Applied Sciences, MU S T, Mongolia*
16.15-17.15	**Poster Session and Coffee break**
19.00	**Conference banquet**

03 October, 2024

(Conference Hall #502, Library, National University of Mongolia)

Chairperson: Prof. Altan Bolag	
09.00-09.30	**Invited talk by Prof. Bai Narsu** *Inner Mongolia Normal University, China* Computational design and property tailoring of MgSc alloys
09.30-10.00	**Invited talk by Prof. A. Nomoev** *Institute of Physical Material Science SB RAS, Russia* Microwave absorption of composite with high content of carbonyl iron microparticles
10.00-10.15	A study of size dependences of melting temperature of various types of Pd-Si nanoparticles using the molecular dynamics method **D.G. Tsydypov** *Institute of Physical Material Science of the Siberian Branch of the Russian Academy of Sciences, Russia*
10.15-10.30	*Ab initio* calculations on electronic properties of Trans-4-(trifluoromethyl) cinnammic acid **N. Naranbilegt** *Laser research center, National University of Mongolia*
10.30-10.45	Crystal structure and optical properties of semiconductor WO_3 **B. Nomin** *Institute of Physics and Technology, Mongolian Academy 0f Sciences, Mongolia*
10.45-11.00	Morphological influence of the silver gas diffusion electrode on the selectivity of electrochemical CO_2 reduction **M. Batpurev** *Department of Physics, National University of Mongolia, Mongolia*
11.00-11.30	**Coffee break**

Chairperson: Professor A.Nomoev	
11.30-12.00	**Invited talk by Prof. Altan Bolag** *Inner Mongolia Normal University, China* Organic-inorganic composite materials in solar cells and lithium-ion batteries
12.00-12.30	Repair of waste lithium iron phosphate **Wei Li** *Inner Mongolia Normal University, China*
12.30-12.45	Antioxidant activities of aqueous extracts from Mongolian wild berries and their biosynthesized silver nanoparticles **Ts. Bolor** *Institute of Chemistry and Chemical Technology, Mongolian Academy of Sciences, Mongolia*
12.45-13.00	The influence of the concentration of copper and zinc in the melt on the formation of various phases of brass nanoparticles **E.Ch. Khartaeva** *Laboratory of Composite Materials Physics, Institute of Physical Material Science of the Siberian Branch of the Russian Academy of Sciences, Russia*
13.00-13.15	Synthesis and characterization of $BaFe_{12}O_{19}/Mg_{0.4}Ni_{0.6}Fe_2O_4$ bicomposite **I. Khishigdemberel** *Institute of Physics and Technology, Mongolian Academy 0f Sciences, Mongolia*
13.15-13.30	**Discussion & Closing**

Poster Presentations

№	Authors	Presentation Title
1	M.V.Korolkov, I.A.Khodasevich, A.S.Grabtchikov, G.Munkhbayar, D.Mogilevtsev	Verification and spectral separation of up-conversion luminescence processes in fluorophosphate glass doped with ytterbium and thulium ions by effective nonlinearity of up-conversion processes
2	D.Naranchimeg, S.Ochir, G.Munkhsaikhan	Calculation of doubly excited states of the helium atom using the Hartree-Fock method
3	N.Kalanda, M.Yarmolich, A.Petrov, A.Normirzaev, M.Tukhtabayev, D.Sangaa and S.Munkhtsetseg	Obtaining high-density strontium-substituted ferromolybdate targets
4	B.Batgerel, M.Chagdarjav, N.Jargalan	Investigation of the aggregation of fullerenes C_{60} in water/NMP mixtures by molecular dynamics simulation
5	G.Munkhbayar, D.Unurbileg, Kh.Tsendsuren, N.Tuvjargal, J.Davaasambuu	Supercontinuum generation from thin plates
6	Wurentuya Bhnar, Ren Wu, Agula Bao	Lignocellulose composition of preparation of porous carbon materials and CO_2 adsorption performance research
7	Bao Siriguleng, Gong Lingzhen, Bao Agula	Preparation and characterisation of urea-modified lignin-derived porous carbon materials and their CO_2 adsorption properties
8	Deng Lili, N.Tuvjargal, N.Tsogbadrakh and J.Davaasambuu	Experimental studies of structural and optical properties of Nd-doped $LiYF_4$ compounds
9	Jiayu Li, Tana Bao, Altan Bolag, Narengerile, Yin Gang and O. Tegus	Preparation and characterization of carbon aerogel by freeze-drying method
10	Anqi Wang, Gerile Naren, Liang Jun Wu, FangYi Xu, Wei Wei	Synthesis of luminescent matrix materials of rare earth Tb and Eu and its basic application in OLED devices
11	Gerile Naren, Zihao Qiu, Aorigele Bohnuud, Rui Meng,Tana Bao	Study on the structural and photophysical properties of N-acyl amino acid europium complexes
12	B.B. Damdinov, A.I.Lyamkin, V.A.Prigozhikh	Modeling of sound propagation in liquid medium depending on the size of air bubbles
13	Lygdenov Valery, Bardakhanov Sergei, Nomoev Andrey, Syzrantsev Vyacheslav	Determination of thermal conductivity of silica dioxide tarcosil T-50 nanopowder by laser flash technique
14	A.S.Milonov, U.L.Mishigdorzhiyn,	Features of the formation of protective layers of chromium borides on the surface of die steels

	S.A.Lysykh, Yu.I.Semenov, and M.Yu.Kosachev	
15	Stepan Lysykh, Undrakh Mishigdorgiin, Alexandr Milonov, Vasilii Kornopoltsev	Investigation of multifunctional diffusion layers created on the surface of iron-carbon alloys by combined methods of chemical-thermal treatment and electron beam treatment
16	Tatiana Grigorieva, Yauheni Auchynnikau, Yahenia Eysimont	Reactive plastic materials modified by mechanically activated particles
17	Y.Auchynnikau, V.Mikhailov, A.Svistun, D.Linnik, Y.Matuk, A.Auchynnikau	Physical and mechanical characteristics of electrospark coatings
18	Nikolai Chekan, Igor Akula, Yauhenia Eisymont, Aleksei Auchynnikay	High-entropy vacuum coatings
19	Alexandr Voznyakovsky, Alexey Voznyakovsky, Yauheni Auchynnikau, Yauhenia Eisymont	Graphene-containing polymer materials
20	J.Vanchinkhuu, M.I.Markevich, Ts.Erdenebat , G.Buyantsetseg	Thermogravimetric and BET analysis on discharge products
21	Kh.Tuvshin-Erdene	Chemical composition determination of black fingerprint powders
22	Amartuvshin Oidov, Dovchinvanchig Maashaa	Research on the seed peeling process on bull-dect equipment
23	Munkhjargal Badamdorj, Dovchinvanchig Maashaa	Microstructure, phase transformation and mechanical properties of Ni-Ti-Hf-La alloys
24	Bolormaa Dorjsuren, Dovchinvanchig Maashaa	Effect of La addition Microstructure and Mechanical Property of Ti-Nb-La alloys
25	Sarantsetseg. P, Davaabal. B, Bayarzul. U, Narandalai. B, Nyamdelger. Sh, Oyun-Erdene. G, Enkhtuul. S	Characterization of geological materials from the Baganuur coal mine area
26	O.Erdenetuya, B.Odontuya, Yu.Ganchimeg, E.Gurbadam, S.Jargalan, D.Otgonbayar, G.Batdemberel, D.Jamiyanaa, J.Battogtokh, G.Munkhsaikhan	Liquid phase exfoliation of MoS2 in aqueous IPA
27	N.Togtokh, B.Ikhbayar, L.Sarantuya, A.Munkhbaatar, G.Sevjidsuren	Recovering possibilities of REEs from spent NiMH in Mongolia using hydrometallurgical methods
28	B.Ikhbayar, N.Togtokh, L.Sarantuya, A.Munkhbaatar, G.Sevjidsuren	Possible application of Ni microparticles recovered from spent NiMH batteries for water splitting and green energy technologies
29	A.G.Anisovich, M.I.Markevich,	Obtaining carbon nanoparticles by pulse laser influence in a double-pulse mode in an aquatic environment

	V.I.Zhuravleva, Zh.Vanchinhuu, Ts.Sainsanaa	
30	A. S.Piotukh, E.V.Kolobkova, V.A.Orlovich, I.A.Khodasevich	Fluorophosphate glass for fluorescence thermometry: optimization of holmium and ytterbium ions concentration
31	R.V.Chulkov, J.Davaasambuu, G. Shilagardi, L.Batay, A.S.Grabtchikov, A.I.Vodchits, V.A.Orlovich	SRS in compressed hydrogen by two-pulse biharmonic pump: modeling and experiment
32	Chimytov Timur, Kalashnikov Sergey, Nomoev Andrey	Dielectric properties of liquid crystals in porous media
33	G.Davaadulam, T.Begzsuren, D.Usukhjargal, T.Badamkhatan	Optical characterization of Rosa baitagensis leaves cultured *in vitro*
34	Gantumur Tsend, Chen Qicheng	Effect of deposition on heat transfer enhancement using nanofluids on microscopic mechanism by molecular dynamics
35	P.L.Abiduev, T.G.Darmaev	Approximate temperature fields in two-layer cylinder at pulse thermal loading
36	G.Narkhajid, S.Baasanjargal, S.Enkhtur, D.Rentsenmyadag, Ts.Ninjbadgar, G.Erdene-Ochir, S.Munkhtsetseg	Preparation and characterization of new porous carbon material from cow manure using pyrolysis
37	M.Uyanga, B.Buyankhishig, D.Rentsenmyadag, T.Murata, J.Batkhuu	Research on the chemical composition and biological activity of Artemisia scoparia Waldst. et Kit.
38	S.A.Nomoev, I.S.Vasilevskii	A Proposal of Mach-Zehnder Interferometer
39	E. M.Shpilevsky, O.G.Penyazkov, S.A.Filatov, G.Shilagardi, D.Ulam-Orgikh, S.Munkhtsetseg	Spectral methods in the study of metal-fullerene films
40	S.P.Bardakhanov	Fine powders and advanced materials
41	Chingis Gulgenov, Ivan Simakov, Sayana Bazarova and Ksenia Artem'eva	Determination of dielectric properties of liquid in nanoscale layer
42	Maria Parfenova, Vera Vorob'eva, Vasily Lutsyk, Anna Zelenaya	Elimination of Contradictions in the Phase Diagrams of Ternary Systems Sb-Sn-M (M=Ag,Bi,In,Ga,Zn) by the 3D Computer Models

Characterization of low- and high-calcium pond ashes and their applicability for the preparation of alkali-activated pastes

Jadambaa Temuujin[1] and Uyat Bayarzul[2]

[1]*CITI University, Denver Street 34, Ulaanbaatar 14190, Mongolia*
[2]*Institute of Chemistry and Chemical Technology, Mongolian Academy of Sciences, Ulaanbaatar, Mongolia*

Email: temuujin.jadamba@citi.edu.mn

Depending on the collecting methods, coal combustion by-products are usually divided into fly ash, bottom ash, and flue gas desulfurization product. Because they are a hazardous dust source, they are often stored underwater in ponds or lagoons and are called pond ash.

In this investigation, the pond ashes from Ulaanbaatar's 4th TPS (thermal power station) and Erdenet's TPS were characterized by XRF, XRD, BET, PSD, SEM and TEM. The pond ash of the 4th TPS contains more than 20% calcium oxide, while Erdenet's TPS contains around 4% calcium oxide. PSD of the 4th TPS shows a bimodule distribution with a maximum of 36 and 260 mm, while Erdenet's pond ash shows an unimodal distribution with a maximum of 74 mm. The main crystalline compounds of the 4th TPS pond ash were quartz, calcite, hematite, albite, and akermanite, while in the Erdenet pond ash were quartz, mullite, magnetite, and calcite. The mineralogical composition of the pond ashes depends on the used coal type, the power plant's working principle and the duration of time inside the ash pond.

The alkali-activated binder prepared from these pond ashes demonstrated a weak compressive strength of around 1.5-2.5 MPa after 7 days. Notably, the high-calcium pond ash-based alkali-activated paste exhibited slightly higher mechanical properties than the low-calcium pond ash-based paste. The weak mechanical properties of the pond ash-based alkali-activated materials are related to both pond ashes' porous and high-surface microstructure. High calcium pond ashes could exhibit a partial calcium silicate formation reaction, which is the reason for the higher mechanical properties than low calcium pond ash-based alkali-activated pastes. Furthermore, a brief mechanical activation of these pond ashes for 20 min slightly improved their mechanical properties, reaching up to 3.75 MPa.

Keywords: Coal types, Pond ashes, Chemical and Mineralogical composition, Microstructure, Alkali-activated paste, Mechanical properties

Maze balls and metabeams: how to stop sound in its tracks

O. B. Wright

Graduate School of Engineering, Osaka University, Yamadaoka 2-1, Suita 565-0871, Osaka, Japan
Hokkaido University, Sapporo 060-8628, Japan

Email: olly@eng.hokudai.ac.jp

Controlling sound with acoustic metamaterials is a booming subject in every sense of the word. Here we present two studies on stopping sound using metamaterial structures. In the first study we propose an octagonal onion-like structure with interconnected labyrinthine shells that can reflect sub-kHz airborne sound when placed inside a cylindrical tube. The structure, fabricated by 3D printing, is found to stop 67% of the incident sound on resonance with a volume filling fraction of only 13%. In the second study we propose metabeams that can stop all polarizations of sound, that is longitudinal, shear and torsional, travelling down them in the region of the kHz metamaterial band gap. Potential applications include sound and vibration control.

References

[1] 'Compact acoustic metamaterial based on the 3D Mie resonance of a maze ball with an octahedral structure', T. Zhang, E. Bok, M. Tomoda, O. Matsuda, J. Guo, X. Liu, and O. B. Wright, Appl. Phys. Lett. 120, 161701 (2022)

[2] 'Tapered rainbow metabeam for wideband multimode acoustic blocking based on quadruple-mode resonators', H. Takeda, E. Murakami, M. Tomoda,1 O. Matsuda, K. Fujita, and O. B. Wright, Appl. Phys. Lett. 121, 131701 (2022)

[3] 'Wave-canceling acoustic metarod architected with single material building blocks', A. Ogasawara, K. Fujita, M. Tomoda, O. Matsuda, O. B. Wright, Appl. Phys. Lett. 116, 241904 (2020)

[4] 'Perfect acoustic bandgap metabeam based on a quadruple-mode resonator array', K. Fujita, M. Tomoda, O. B. Wright and O. Matsuda, Appl. Phys. Lett. 115, 081905 (2019)

Possibility of Detection of Hepatitis D Virus Using Surface Plasmon Resonance

Batzul Ganbold[1], Galbadrakh Ragchaa[1], Bolorchimeg Jamsran[1], Naranbat Baasankhuu[1], Odgerel Oidovsambuu[2], Davaasambuu Jav[1]

[1]Electronics and Photonics Laboratory, Institute of Physics and Technology, Mongolian Academy of Sciences
[2]National University of Mongolia, Ulaanbaatar, Mongolia

Background: Hepatitis D Virus (HDV) presents a significant medical concern in Mongolia. Traditional diagnostic methods, such as ELISA and PCR, are time-consuming and requires labeling. In contrast, Surface Plasmon Resonance (SPR) biosensors offer high sensitivity to refractive index changes, require less time, and enable real-time detection.[1]
In this research, SPR is excited by He-Ne laser which impinges on gold thin film through a BK7 glass prism. (Figure 1). When the incident light and surface plasmons are phase matched, the wave vectors are expressed as:

$$k_x^{pr} = k_x^{spr}$$

$$\frac{\omega}{c}\sqrt{\varepsilon_{pr}}\,sin(\theta) = \omega/c\sqrt{\frac{\varepsilon_1\varepsilon_2}{\varepsilon_1+\varepsilon_2}} \rightarrow \theta_{SPR} = sin^{-1}\sqrt{\frac{\varepsilon_1\varepsilon_2}{\varepsilon_{pr}(\varepsilon_1+\varepsilon_2)}}$$

In the above equation, the dielectric constants of prism (ε_{pr}), and gold (ε_2) are constant, ε_1 is dielectric medium on the surface of gold thin film.[2]. If ε_1 varies as different medias, there is a shift in SPR angle. This sensitivity to changes of refractive index allow us to detect the HDV virus.
Experimental methods: Approximately 50 nm gold thin film is deposited on glass substrate via ion sputtering. We immobilize a solution of antigen S-HDAg that on the surface of gold thin film and treat it with negative (negative serum sample) and positive (positive serum sample) sample solutions. In total, 36 samples (18 negative, 18 positive) were prepared and analyzed.
Due to S-HDAg binding with positive sample, it causes the significant SPR angle shift, while negative sample causes less.
Results: Over 20 minutes, our SPR instrument, based on He-Ne laser, measures the intensity that reflected from an immobilized sample on the surface of gold thin film from 35° to 60°. The angle with the lowest measured intensity was selected as the SPR occurrence angle.

From the average value, the angle that SPR occurred at were: gold thin film at 45.8°, S-HDAg at 48.4°, the negative sample at 49.7° and the positive sample at 52.4°. (Figure 2).

Conclusion: These results demonstrate that SPR biosensor is able to detect HDV virus accurately in short time.

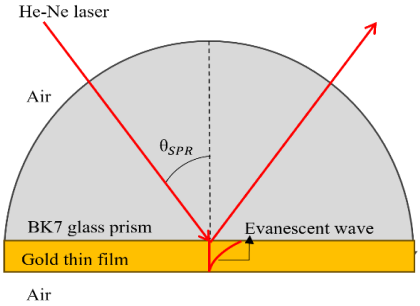

Figure 1. Exciting surface plasmon polaritons. Kretchman configuration.

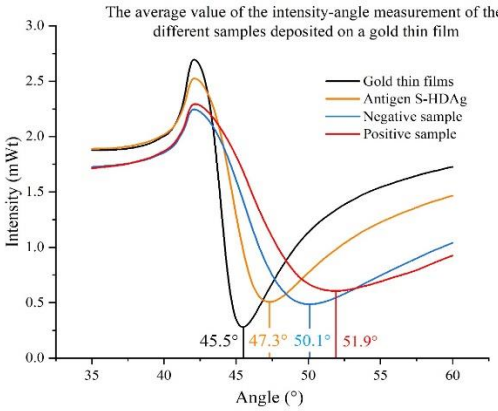

Figure 2. The average value of the intensity-angle measurement of the different samples deposited on a gold thin film.

References:

[1] Номин, А., Номин-Эрдэнэ, Э., Бадмааараг М., Хулан, Н., Эрдэнэ, Н., & Одгэрэл, О. (2021). Хепатитийн дельта вирүсийн халдварыг илрүүлэх гадаргуугийн плазмон резонанс дээр үндэслэсэн оношлуурыг зохион бүтээх. Mongolian Journal of Engineering and Applied Sciences, 3(1), 25–34. https://doi.org/10.22353/mjeas.v3i1.36.

[2] Nomin-Erdene, E., Khos-Ochir, T., Tuvjargal, N., Munkhbayar, G., Davaasambuu, J., Nomin, A., & Oidovsambuu O. (2020). Thickness Optimization of a Mono Metallic Plasmonic Structure for a Surface Plasmon Resonance Biosensor. Scientific Transaction of the National University of Mongolia. Physics, 31(536), 1-5.

Surface properties of the mechanical exfoliated MoS2 few layers

B.Odontuya[1,a], D.Otgonbayar[1,b], O.Erdenetuya[1,c], G. Batdemberel[1,d], E. Gurbadam[2,e], S.Jargalan[2,f], D. Jamiyanaa[3,g], J. Battogtokh[4,h] and G. Munkhsaikhan[1,i*]

[1]*Department of Physics, School of Applied Sciences, Mongolian University of Science and Technology, Ulaanbaatar, Mongolia*
[2]*Center for Technology Minerals and Innovation, School of Geology and Mining Engineering, Mongolian University of Science and Technology, Ulaanbaatar, Mongolia*
[3]*Science Department, Chatham University, Pittsburgh, Pennsylvania, USA*
[4]*Jacobs Engineering Group, Hanover, Maryland, USA*

Email: gmunkhsaikhan@must.edu.mn

In this work, the surface morphology of MoS_2 has been investigated. Atomic-resolution images of bulk MoS_2 were obtained using a scanning tunneling microscope. Two types of atomic defects were identified as defects in the molybdenum atomic layer directly below the topmost sulfur layer. Studies to determine the layers mechanically exfoliated MoS_2 have been carried out using an optical microscopy, an atomic force microscopy, and resonant Raman spectroscopy. Flakes from ten to many layers detected by AFM analysis. In parallel, a systematic resonant Raman investigation was performed, ranging from ten layers to the bulk MoS_2, clearly showing systematic layer-dependent spectral features.

Keywords: Layered materials, surface defects, impurities, STM, AFM, resonant Raman spectroscopy, layer identification in 2D materials, MoS_2.

Tailoring Martensitic transition of MgSc alloys by vacancy defects

Narsu Bai, Jiaxin Li and Xiaoxia Wu

Inner Mongolia Key lab of Physics and chemistry of functional materials, Inner Mongolia Normal University, 010022, Hohhot China
College of Physics and electronic information, Inner Mongolia Normal Uni versity, 010022, Hohhot China

Email: nars@imnu.edu.cn

MgSc alloys are regarded as promising new lightweight shape memory alloy materials due to their low density and high specific strength. It has been found that the β single-phase MgSc alloys that undergo thermoelastic martensitic transformation between the β and α″ (orthorhombic) phases have shape memory effect and superelasticity [1-3]. However, current studies show that the martensitic transformation temperature of MgSc alloys is very low, which limits the application of the alloys to a certain extent. In previous experiments, in order to ensure the shape memory effect, the minimum Sc content in MgSc alloys was 18.3%. However, the maximum temperature of Mg-18.3% Sc alloy was as low as -30°C [1]. This is actually because there is no energy barrier between the austenite phase (bcc) and the martensite phase (orthogonal) of Mg-18.75 at.%Sc [4,5]. Recently, Tripathi et al. demonstrated through DFT [6] that an appropriate amount of interface strain can increase the transformation temperature to room temperature. However, this method is difficult to achieve in experiments. Therefore, increasing the transformation temperature of magnesium-scandium alloys by simple and effective methods remains a major problem. In this work, we propose that vacancies have an important influence on stabilizing the bcc phase, increasing the phase transition energy barrier, and thereby increasing the martensitic phase transition temperature.

The significant effect of vacancies on the bcc phase MgSc alloy is confirmed through first-principles calculations of lattice dynamics and minimum energy paths. In the bcc phase $Mg_{39}Sc_9$ (18.75% Sc) alloy, the appearance of vacancies eliminated the imaginary frequencies in the phonon spectrum, thereby generating the dynamically stable bcc phase $Mg_{38}Sc_9Va_1$ alloy. When there was a single point defect in the bcc structure, $Mg_{38}Sc_9Va_1$ with different vacancy positions all exhibited lattice dynamic stability, as shown in Figure 1b. Compared with $Mg_{39}Sc_9$ in Figure 1a, the acoustic spectrum frequency of the $Mg_{38}Sc_9Va_1$ alloy significantly hardened. Particularly in the region around the X direction, the frequency was at least 0.75 THz higher than the frequency at the

corresponding position of the $Mg_{39}Sc_9$ alloy. This indicates that monovacancy prevents the relative slip of atomic layers of the bcc structure in the b direction, thereby forming a stable bcc phase MgSc alloy.

In the 108 atom bcc phase $Mg_{87}Sc_{21}$ alloy with vacancy concentration of only ~0.9%, the appearance of vacancy eliminates the imaginary frequency in part of the structure, while the $Mg_{86}Sc_{21}Va_1$ alloy with imaginary frequency is still bcc phase due to the appearance of energy barrier in the phase transition path. For $Mg_{38}Sc_{10}$ (20.83 at.%Sc) alloy with high Sc composition and stable lattice dynamics, the existence of vacancy has a significant effect on the phonon behavior of MgSc alloy, indicating that the monovacancy has an inevitable effect on the dynamical stability of bcc phase. The monovacancy hardens the acoustic branches of the bcc phase, resulting in a more stable MgSc austenite. It is well known that the higher energy barrier in the phase transition path is key to the increase of the martensitic transition temperature. Therefore, vacancy is an important way in raising the transition temperature.

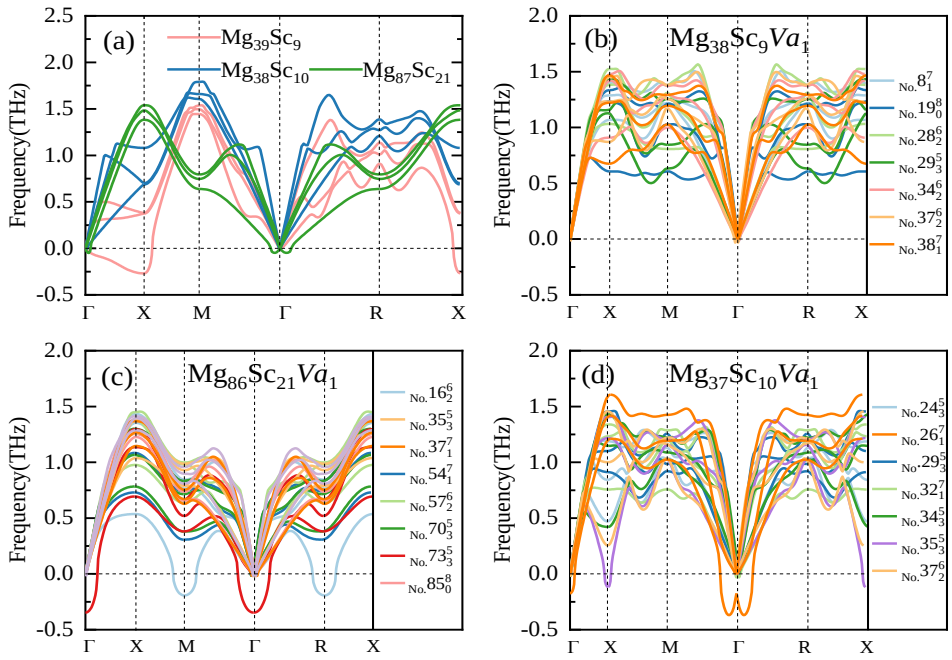

Fig. 1. Effect of different Vacancy configuration on the Phonon dispersion.

References

[1] Y. Ogawa, D. Ando, Y. Sutou, J. Koike, A lightweight shape-memory magnesium alloy, Science, 353(2016)368-370

[2] Y. Ogawa, D. Ando, Y. Sutou, H. Somekawa, J. Koike, Martensitic Transformation in a β-Type Mg–Sc Alloy, Shap. Mem. Superelasticity, 4(2018)167–173.
[3] K. Yamagishi, Y. Ogawa, D. Ando, Y. Sutou, J. Koike, Room temperature superelasticity in a lightweight shape memory Mg alloy, Scripta materialia, 168 (2019)114–118.
[4] W. Zhao, K. Zhang, E. Guo, L. Zhao, X. Tian, C. Tan, Martensitic transformation mechanism of Mg-Sc lightweight shape memory alloys, Scripta Materialia, 207 (2022)114316.
[5] J. Li, X. Wu, L. Li, N. Bai, Lattice dynamics of Mg-Sc lightweight shape memory alloys, Journal of Alloys and Compounds, 976 (2024) 173303.
[6] S. Tripathi, K. G. Vishnu, M. S. Titus, A. Strachan, Tunability of martensitic transformation in Mg-Sc shape memory alloys: A DFT study, Acta Materialia 189 (2020) 1-9.

Microwave Absorption of Composite with High Content of Carbonyl Iron Microparticles

Andrey Nomoev, Bair Garmaev, Ilya Yuzhakov and Damdin Tzydypov

Institute of the Physical Materials of the Siberian Branch of the Russian Academy of Sciences

Email: nomoevav@mail.ru

The developed technique for creating silicone composites with a high concentration of carbonyl iron micropowders makes it possible to obtain materials with high electromagnetic parameters. The use of mechanical stirring and pressing provides the material with magnetic properties. Despite the high concentration, above 80 wt.% carbonyl iron, the samples do not conduct electric current. With increasing concentration of carbonyl iron in the composite, electromagnetic losses increase. The highest absorption value of electromagnetic radiation from 10% to 50% at frequencies of 1-6 GHz is observed for samples containing P10 micropowder. For composite samples, interactions with the electromagnetic field are increasing within the error limits. The values of reflection coefficients increase monotonically from 0% to 20% in the frequency range under study. Magnetic permeability was calculated using a developed program for calculating the frequency dependences of complex values of dielectric and magnetic permeability [1].

References

[1] Certificate of state registration of a computer program No. 2024618769 Russian Federation. Program for calculating frequency dependences of complex values of dielectric and magnetic permeability of materials: No. 2024617388: application. 04/08/2024: publ. 04/17/2024 / B. Z. Garmaev, E. Yu. Korovin, A. V. Nomoev, E. B. Atutov; applicant Federal State Budgetary Institution of Science Institute of Physical Materials Science of the Siberian Branch of the Russian Academy of Sciences.

A Study of Size Dependences of Melting Temperature of Various Types of Pd-Si Nanoparticles Using The Molecular Dynamics Method

Damdin Tsydypov, Andrey Nomoev and Bair Garmaev

Institute of the Physical Materials Science of the Siberian Branch of the Russian Academy of Sciences

Email: damdinkatsydypov@gmail.com

Metal-semiconductor nanoparticles have recently begun to attract great interest due to the wide range of possible applications. This interest is related to the development of probe methods for studying semiconductor structures, the development and manufacture of nanoscale Schottky contacts for microwave and terahertz applications [1]. In this paper, a computer simulation using the molecular dynamics method was carried out to study the size dependences of the melting temperature of various types of Pd-Si nanoparticles. Based on the temperature dependences of the potential part of the internal energy of the Pd-Si nanoparticle, the size dependences of the melting temperature were constructed and analyzed. Also, the size dependences of the melting temperature obtained by us were compared with the results of previous investigations devoted to modeling the melting of composite nanoparticles.

References

[1] N.V. Vostokov, V.I. Shashkin, *Semiconductors*, 9, 1084 (2004).

Ab initio calculations on electronic properties of Trans-4-(trifluoromethyl) cinnammic acid

N.Naranbilegt[1, 3], A.Munkhbaatar[1] U.Bayasgalan[2], B.Khongorzul[2], J.Davaasambuu[1, 3]

[1] *Institute of Physics and Technology of Mongolian Academy of Sciences*
[2] *Institute of Chemistry and Chemical Technology of Mongolian Academy of Sciences*
[3] *Laser Research Center of National University of Mongolia*

We have performed ab-initio calculations on relatively new type of molecular crystal "trifluoromethyl cinnamic acid" with chemical composition $C_{10}H_7F_3O_2$. The molecular crystal was grown in laboratory environment and then we have done x-ray diffraction measurement to determine its crystal structure. After conducting measurement, its crystal structure was determined to be triclinic and space group number was 2, which is P-1. The specimen had total of 44 atoms in its unit cell and lattice parameters were 7.8 Å, 7.9 Å, 14.9 Å, which is moderately sized crystal. To perform these calculations, we used the Quantum Espresso Package, which was enough for our desired results. We first did relaxation to accurately determine the positions of the atoms in the cell, then from Self-Consistent-Field to non-SCF, in order. We employed a plane wave (PW) basis set due to its numerous advantages. The plane wave basis set allows for systematic control over the accuracy of our calculations by adjusting the kinetic energy cutoff, ensuring reliable and convergent results. Given the periodic nature of our triclinic crystal, plane waves seamlessly handle periodic boundary conditions, simplifying the computational setup and reducing complexity. By combining plane waves with UPF pseudopotentials, we efficiently model the core electrons of heavy atoms such as fluorine, optimizing the balance between computational cost and accuracy.

After that, we calculated the density of the states and evaluated the band gap between conduction band and valence band and how each atomic orbitals make up it. The specimen had band gap value of 2.7 eV which tell us that it is indeed semiconductor type material. To complement the findings, we also assessed the electronic band structure of the system. Triclinic is known for its notoriously low symmetry compared to others and few high symmetry points were taken into account. We have deemed those symmetry points Γ—X|Y—Γ—Z|R2 were sufficient for our calculation and choose 49.1 Ry for kinetic-energy cutoff, 442.3 Ry for charge density cutoff.

Keywords: solid-state calculation, electronic properties, crystal

Crystal structure and optical properties of semiconductor WO_3

Nomin B*, Munkhbaatar A, Bolormaa B, Bumaa B, Nyamdavaa E and Sevjidsuren G

Institute of Physics and Technology, Mongolian Academy of Sciences, Peace Avenue 54b, Ulaanbaatar 13330, Mongolia

*Email: Nomin_b@mas.ac.mn

In recent years, hydrogen energy has been extensively studied to reduce greenhouse gas emissions. Hydrogen energy represents a great potential solution to meet global energy demand. It is gaining attention for some reasons as clean, versatility, decarbonization, and energy security. Hydrogen is widely used in fuel cells and internal combustion engine applications. Therefore, its purity needs to be high quality. To produce hydrogen with high purity by water electrolysis, the catalytic activity of the catalysts should be high [1,2]. Nickel and its alloys are studied in the process of hydrogen evolution in alkali. However, nickel has low catalytic activity compared to expensive catalysts such as platinum (Pt), iridium (Ir), and rhodium (Th). To increase the catalytic properties of nickel, combining with other metals, non-metals and mixing with carbon matrix [3-5]. We aimed to improve the catalytic properties of nickel by doping with semiconductor tungsten oxide (WO_3).

In this work, the structural properties and bandgap behavior of WO_3 samples were presented. Figure 1.(a) compares the XRD result of the WO_3 sample synthesized by hydrolysis and dried at 100℃ (black), and the XRD result after rewashed with water and calcinated at 450℃ (red). The XRD result shows that the sodium chloride impurity phase was removed after washing and monoclinic WO_3 was formed after calcination. Figure 1.(b) shows a comparison of the UV-vis spectra of the samples. In Figure 1.(c), using first-principles methods, it was shown that the WO_3 material exhibits semiconductor behavior with a bandgap of 1.2 eV and 1.5 eV using the GGA and GGA+U calculations respectively.

Keywords: Tungsten oxide (WO_3), catalysts, bandgap, DFT+U

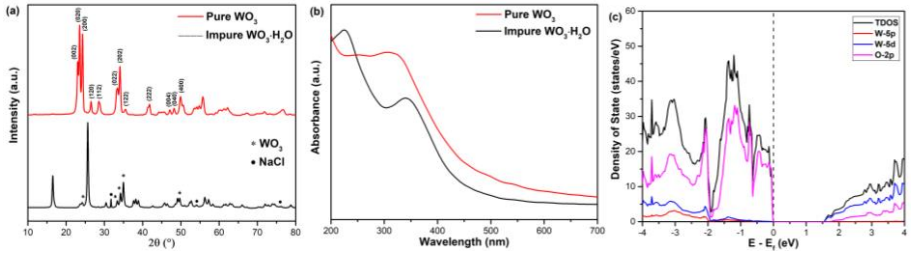

Fig. 1. (a) XRD, (b) UV-vis spectra and (c) GGA and GGA+U calculations of WO_3

References

[1] Yue, Meiling, et al., *Renewable and Sustainable Energy Reviews*, 146, 111180 (2021).
[2] Monir, Minhaj Uddin, et al., *Renewable Energy and Sustainability Elsevier*, 299-325 (2022).
[3] Oshchepkov, Alexandr G, et al., *ACS Catalysis 10, 13*, 7043-4068 (2020).
[4] S.M.A. Shibli, et al., *Int. J. Hydrogen Energy*, 41, 10090 (2016).
[5] A. Maizelis, B. Bairachniy., *Springer Nature Singapore*, 97-107 (2019).

Morphological influence of the silver gas diffusion electrode on the selectivity of electrochemical CO_2 reduction

Batpurev M.[1,3], Amarbayar A.[2], Nakano Y.[3], Erdene-Ochir G.[1]

[1]*Department of Physics, National University of Mongolia*

[2]*School of Engineering and Technology, National University of Mongolia*

[3]*The University of Tokyo, Japan*

E-mail: batpurevm@gmail.com

Electrochemical reduction of CO_2 is attracting attention as a CO_2 conversion method which can use renewable energy on a large scale. Silver (Ag) is a well-known electrocatalyst for carbon monoxide (CO) production through CO_2 reduction. CO_2 reduction with Ag-based electrocatalysts has been mainly studied using H-type cell under CO_2 ambient. However, the reaction rate has been limited due to the low solubility of CO_2 to water. Recently, there are many reports on gas diffusion electrode (GDE) as cathode for CO_2 reduction because it can increase current density largely, but the number of reports on Ag-based GDE is limited. Here, we assess the CO_2 reduction activity of Ag electrocatalysts loaded on GDE and evaluated its product selectivity and durability using on-line gas analysis system. In addition, nano-porous Ag was also synthesized and tested, because nanostructured Ag is known to have higher CO_2 reduction activity in comparison with bulk Ag owing to its high surface area.

Study on optimizing properties of lithium-ion batteries based on antraquinone cathode materials

Altan Bolag, Xia Hong, Wenhui Liu and Yanchao Sun

Inner Mongolia Key Laboratory for Physics and Chemistry of Functional Material, College of Physics and Electronic Information, Inner Mongolia Normal University

Email: 20214016028@mails.imnu.edu.cn
Email: altan.bolag@imnu.edu.cn

Organic conjugated oxygen-containing compounds, especially anthraquinone derivatives, are considered promising cathode materials for lithium-ion batteries due to their high theoretical capacity, environmental friendliness, and strong structural designability. However, optimizing the capacity, platform voltage, cycle stability, and rate performance of batteries through molecular structure design remains a key challenge for researchers.

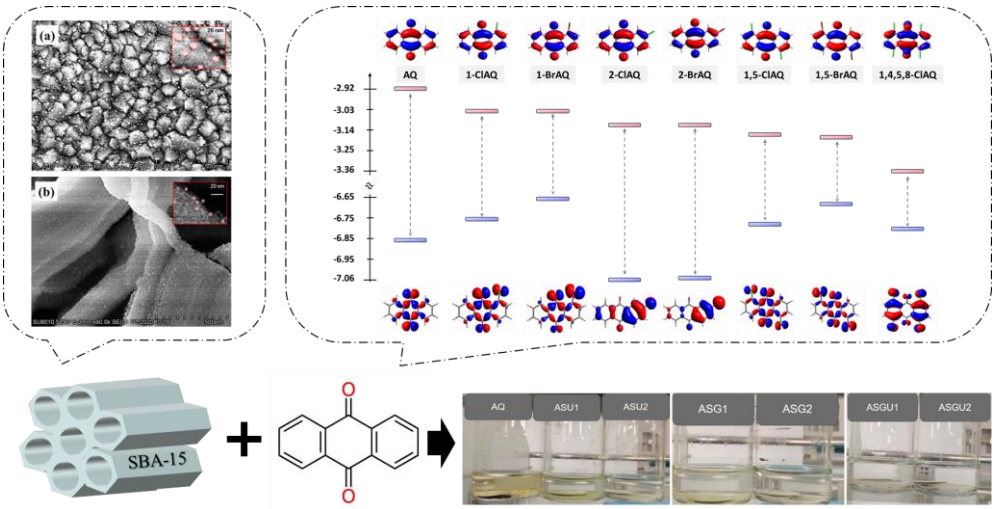

Fig. 1. Study on optimizing properties of lithium-ion batteries based on antraquinone cathode materials

At the beginning of this research, we studied the remarkable effect of SBA-15 molecular sieves on the dispersion of Pt particles and the number of catalytic active sites, and then systematically studied the impact of SBA-15 molecular sieve on the cycle stability of anthraquinone organic cathode lithium-ion batteries. The study found that by loading anthraquinone through the pore structure of SBA-15 molecular sieve, the cycle life and electrochemical performance of the battery can be

effectively improved, providing a new choice for the cathode materials of lithium-ion batteries. Finally, the study also explored the impact mechanism of different halogen electron-withdrawing groups on the performance of organic cathode materials for lithium-ion batteries. By systematically introducing halogen functional groups of different types, quantities, and positions, the study examined their effects on molecular structural characteristics, physicochemical properties, and battery performance, screening cathode materials that can significantly enhance the performance of lithium-ion batteries and clarifying the impact mechanism of electron-withdrawing groups on the performance of cathode materials.

In summary, this project not only provided in-depth insights into the impact of electron-withdrawing groups on the performance of organic cathode materials but also offered theoretical foundations and experimental support for the development of new high-performance organic cathode materials, opening up new avenues for the performance optimization and material selection of lithium-ion batteries.

References

[1] Lu Y, Zhang Q, Li F, et al. Emerging Lithiated Organic Cathode Materials for Lithium-Ion Full Batteries. Angewandte Chemie International Edition [J]. 2023, 62: 16-47.

[2] Yang JX, Wang ZP, Shi YQ, et al. Poorly Soluble 2,6-Dimethoxy-9,10-Anthraquinone Cathode for Lithium-Ion Batteries: The Role of Electrolyte Concentration[J]. ACS Applied Materials Interfaces, 2020, 12: 179-7185.

[3] Zhang YS, Murtaza I, Liu D, et al. Understanding the Mechanism of Improvement in Practical Specific Capacity Using Halogen Substituted Anthraquinones as Cathode Materials in Lithium Batteries[J]. Electrochimica Acta, 2017, 224: 622-627.

Repair of waste lithium iron phosphate

Bo Liao, Xiaotao Wang, Han Wu, Wei Li

College of Physics and Electronic Information, Inner Mongolia Normal University, Hohhot 010022, Inner Mongolia, China 2 Inner Mongolia Key Laboratory for Physics and Chemistry of Functional Materials, Hohhot 010022, Inner Mongolia, China 3 Inner Mongolia Engineering Research Center for Rare Earth Functional and New Energy Storage Materials, Hohhot 010022, Inner Mongolia, China

Email: liweisyn@163.com

This work uses oxalic acid assisted combustion method to regenerate waste lithium iron phosphate material, and further improves the specific capacity of regenerated lithium iron phosphate through lithium supplementation. The experimental results show that the specific capacity of sample S1 prepared by oxalic acid assisted combustion method reaches 131 mAh/g at 0.2*C* rate. Based on this, the specific capacity of sample S2 further prepared by lithium supplementation technology reaches 151 mAh/g at 0.2*C* rate. The first Coulombic efficiency of the samples exceeded 92%. The sample after lithium supplementation has better cycling performance, with a capacity retention rate of 99% after 50 cycles, and better cycling stability in the later stage.

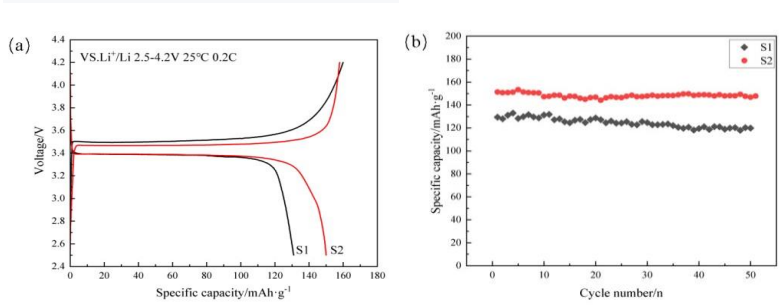

Fig. 1 The first charge-discharge curves (a) and Cycle stability curve (b) of the different samples

References

[1] Y. Li, J. Li, et al. Study on Preparation and Electrochemical Performance of Lithium Iron Phosphate Cathode Ink, Rare metal materials and engineering.51 (2022)3070-3076.

[2] M. Chen, F. M. Liu, S. S. Chen, et al. In situ self-catalyzed formation of carbon nanotube wrapped and amorphous nanocarbon shell coated $LiFePO_4$ microclew for high-power lithium ion batteries[J]. Carbon, 2023, 203: 661-670.

Antioxidant activities of aqueous extracts from Mongolian wild berries and their biosynthesized silver nanoparticles

Bolor Tsolmon[1,*], Tsetseg-Erdene Tseveglkhasuren[2], Sarangerel Oidovsambuu[1]

Natural product chemistry laboratory, Institute of Chemistry and Chemical Technology, Mongolian Academy of Sciences, 13330, Mongolia
[2] Department of Biology, School of Arts and Sciences, National University of Mongolia, Ulaanbaatar 14201, Mongolia

*Email: bolor_ts@mas.ac.mn

Antioxidant activities and the biosynthesis of silver nanoparticles from plant sources have garnered significant global interest recently due to the need for eco-friendly synthesis methods and alternative antioxidant sources. This study investigated the radical scavenging activity using 1,1-diphenyl-2-picrylhydrazyl radical (DPPH) and 2,2'-azino-bis(3-ethylbenzothiazoline-6-sulfonic acid) (ABTS) assays on aqueous extracts and their biosynthesized silver nanoparticles (AgNPs) from three different Mongolian wild berries: blueberry, seabuckthorn, and cranberry.

AgNPs were characterized by UV-visible spectroscopy and scanning electron microscopy (SEM). The maximum absorption peaks for blueberry (Bb-AgNPs), seabuckthorn (Se-AgNPs), and cranberry (Cr-AgNPs) silver nanoparticles were observed at 410 nm, 445 nm, and 410 nm, respectively. SEM analysis revealed that the average sizes of Bb-AgNPs, Se-AgNPs, and Cr-AgNPs were 32.36 ± 1.23 nm, 28.70 ± 1.38 nm, and 30.51 ± 1.22 nm, respectively, with all particles being spherical in shape. The total phenolic content of the aqueous extracts of blueberry, seabuckthorn, and cranberry were 8.98 ± 0.037, 3.65 ± 0.037, and 6.07 ± 0.049 mg GAE/g, respectively.

Among the extracts, cranberry exhibited the highest antioxidant acti vity in both DPPH and ABTS assays, outperforming blueberry and sea buckthorn extracts. The Bb-AgNPs demonstrated superior antioxidant a ctivity compared to their corresponding extract. Seabuckthorn extract s howed weak antioxidant activity, and Se-AgNPs exhibited even weake r activity. Conversely, both cranberry extract and Cr-AgNPs showed st rong DPPH radical scavenging activity, with Cr-AgNPs exhibiting stro nger ABTS radical scavenging activity than its extract.

These results indicate that a more in-depth study is required toeluci date the chemical profile of the aqueous extracts and the mechanisms underlying the formation of silver nanoparticles from these berries.

Keywords: cranberry, blueberry, seabuckthorn, aqueous extract, silver nanoparticle, biosynthesis, antioxidant.

The Influence of the Concentration of Copper and Zinc in the Melt on the Formation of Various Phases of Brass Nanoparticles

Khartaeva E.Ch.[1], Nomoev A.V.[1], Bardakhanov S.P.[1,2], Zobov K.V.[1,2], Trufanov D.Yu.[2], Gaponenko V.R.[2]

[1]*Institute of Physical Materials Science SB RAS, Ulan-Ude, Russia*
[2]*Institute of Theoretical and Applied Mechanics named after. S. A. Khristianovich SB RAS, Novosibirsk, Russia*

Email: erzhena.har@mail.ru

A series of experiments on the production of brass nanoparticles by gas-phase synthesis were carried out on a unique ELV-6 installation [1]. The difficulty with the formation of brass nanoparticles during the evaporation of a brass ingot is that the melting point of copper is higher than the boiling point of zinc. When copper just reaches the solidus point (transition from solid to liquid), zinc is already actively evaporating.

Calculations of the partial pressure of copper and zinc vapors demonstrate the dependence of the ratio of copper and zinc atoms in the evaporation chamber on temperature. These calculations showed that the necessary pressure of copper and zinc vapors for the formation of brass nanoparticles is created only in a narrow temperature range. Calculation of the zinc and copper content in the alloy makes it possible to create the necessary proportion of metals for the synthesis of brass nanoparticles with a given phase.

References

[1] Khartaeva E.Ch., Bardakhanov S.P., Nomoev A.V., Zobov K.V., Trufanov D.Yu. Nanopowders Created by Irradiating Brass with Relativistic Electrons On the sign of the refractive index for metamaterials, Solid State Phenomena. 2023. V. 30, No. 8.

Synthesis and characterization of $BaFe_{12}O_{19}/Mg_{0.4}Ni_{0.6}Fe_2O_4$ bicomposite

Khishigdemberel Ikhbayar, Uyanga Enkhnaran, Jargalan Narmandakh, Deleg Sangaa

Institute of Physics and Technology, Mongolian Academy of Sciences, Ulaanbaatar 13330, Mongolia

Email: khishigdembereli@mas.ac.mn

Magnetic nanocomposites (NCs) are extremely appealing for a wide range of energy-related technological applications, specifically as building blocks for next-generation permanent magnets. The design of such nanostructures requires precise chemical synthesis methods, which will permit the fine-tuning of the magnetic properties. In this paper, we report a simple but novel aqueous solution based 'one-pot' method for preparation of $Mg_{0.4}Ni_{0.6}Fe_2O_4/BaFe_{12}O_{19}$ nanocomposites consist of hard ferrite-soft ferrite phases. The formation of pure crystallized nanocomposites occurred when the precursor was heat-treated at 900°C for 5 hours. As a result, the composite powders consist of $BaFe_{12}O_{19}$ and $Mg_{0.4}Ni_{0.6}Fe_2O_4$ phases. The average crystallite size of the synthesized nanoparticles which were obtained by sol-gel methods were 65 nm, respectively.

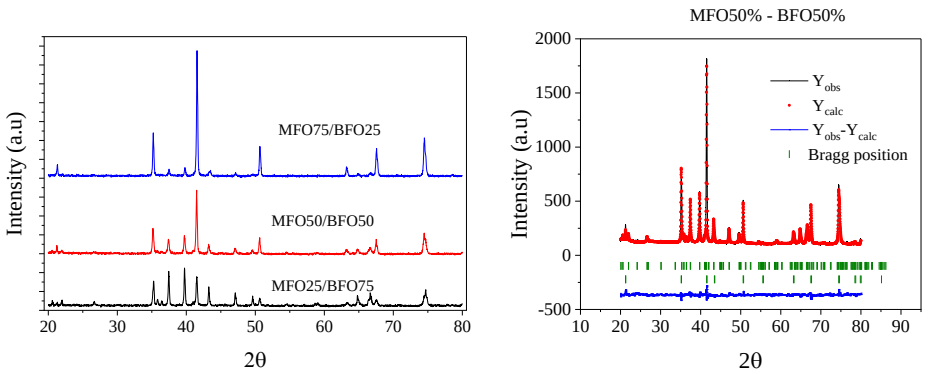

Fig. 1. XRD powder patterns of $BaFe_{12}O_{19}/Mg_{0.4}Ni_{0.6}Fe_2O_4$ nanocomposite ferrites.

References

[1] Pierfrancesco Maltoni, Tapati Sarkar et al., J. Phys. Chem. C 2021, 125, 5927−5936.

[2] Subhenjit Hazra, Barun Kumar Ghosh et al., Journal of Nanoscience and Nanotechnology Vol. 15, 6559–6567, 2015.

Verification and spectral separation of up-conversion luminescence processes in fluorophosphate glass doped with ytterbium and thulium ions by effective nonlinearity of up-conversion processes

M. V. Korolkov[a], I. A. Khodasevich[a],A. S. Grabtchikov[a],
G. Munkhbayar[b], D. Mogilevtsev[a]

[a]*B. I. Stepanov Institute of Physics, National Academy of Sciences of Belarus.*
[b]*Laser research laboratory, School of Arts and Sciences National, University of Mongolia.*

Up-conversion luminescence (UCL) spectra of fluorophosphate glasses doped with the rare-earth ions Yb^{3+} with concentrations of 4% and Tm^{3+} with concentrations of 0.1% were investigated using continuous-wave excitation at 975 nm. For each of four observed UCL bands (near 350, 475, 650 and 800 nm) we observed spectrally overlapping contributions of several up-conversion processes corresponding to the luminescence from various excited states of Tm^{3+}. These states are characterized by different degrees of effective nonlinearity, i.e., different numbers of absorbed photons required to excite these states by transferring energy from the donor Yb^{3+} ions by their relaxation transitions $^2F_{5/2}$ -$^2F_{7/2}$. We also analyzed influence of the pumping power on the contributions to UCL spectra from excitation processes with various effective nonlinearities. We separated the overlapping spectra of compound up-conversion processes different in the degree of effective nonlinearity. Our separation method relies on the factorization of wavelength and pumping power dependencies of the components processes contributions to the total luminescence. The method is self-testing and robust with respect to noise and experimental imperfections. Separating nonlinear processes by pump power dependence means that the spectral components inference can be carried on without a-priori assumptions and/or some preliminary modelling with just a single sample by means of the pump power variation. This separation method is useful when researching nonlinear media aiming for properties necessary for particular applications in sensing/imaging, multi-photon absorption, metrology, etc.

Calculation of doubly excited states of the helium atom using the Hartree-Fock method

D. Naranchimeg[1], S. Ochir[1], G. Munkhsaikhan[1]

[1] *School of Applied Sciences, Mongolian University of Science and Technology, Ulaanbaatar, Mongolia*

Email: naranchimeg@must.edu.mn

In this work we study the double excited states of helium atom. The self-consistent Hartree-Fock (HF) equations double excited states energies for helium atom are solved using the Coulomb Wave Function Discrete Variable Representation approach. The equation is transformed into to a diffusion-type form by an imaginary-time evolution method. Asymptotic solution of these equations reaches to definite energy double excited states. The discrete variable method is used for the uniform and optimal spatial grid discretization and solution of the Hartree-Fock equation. We illustrate that the calculated electronic energies for the helium atom are in good agreement with other best available values.

Keywords: Self-consistent field, imaginary-time, exchange integrals, addition theorem of spherical harmonics.

Obtaining high-density strontium-substituted ferromolybdate targets

Nikolay Kalanda, Marta Yarmolich, Alexander Petrov, Abducaum Normirzaev,Mirzokhid Tukhtabayev, Deleg Sangaa and Sambuu Munkhtsetseg

[1]*Cryogenic Research Division, SSPA "Scientific-Practical Materials Research Centre of the NAS of Belarus", Minsk, Belarus*
[2]*Department of Transport, Namangan Engineering-Construction Institute, Namangan, Uzbekistan*
[3]*Department of Materials Science, Institute of Physics and Technology, Mongolian Academy of Sciences, Ulaanbaatar, Mongolia*
[4]*Department of Physics, School of Arts and Sciences, Natural Sciences Division, National University of Mongolia, Ulaanbaatar, Mongolia*

Email: munkhtsetseg_s@num.edu.mn

The main trends in the production of granular composite films based on multicomponent dielectric/ferrimagnetic/dielectric oxides for nanoelectronic devices are associated with the development of technologies for ion-plasma deposition of composite structures with a given non-stoichiometry deficiency in ferrimagnetic layers and the investigation of their electrical properties. This opens up new opportunities for creating devices with a wide range of applications and high performance characteristics. The use of $Sr_{2-x}La_xFeMoO_{6-\delta}$ films in MRAM cells is predicted as a potential solution to simplify the design of memory and magnetic logic elements. These films will provide a simpler way to create a control local magnetic field, which will facilitate the development of nanoelectronic devices with enhanced capabilities and improved technical characteristics. The properties of magnetoresistive $Sr_{2-x}La_xFeMoO_{6-\delta}$ films strongly depend on the quality and condition of the target used during their deposition. The density, phase homogeneity, and electrical transport properties of the target play a key role in shaping the structural integrity and physical characteristics of the films. Therefore, the goal of this work was to develop optimal modes for obtaining dense single-phase lanthanum-strontium ferromolybdate targets.

The starting reagents for the synthesis of single-phase powder $Sr_{1.5}La_{0.5}FeMoO_{6-\delta}$ (SLFMO) were La_2O_3, Fe_2O_3, MoO_3 and $SrCO_3$. To obtain high-density samples when used as targets for sputtering SLFMO films using various ion-plasma methods, pressing has been employed. The most dense targets without delamination were obtained at a pressing pressure of 2 T/cm^2 using oleates, which are reducing the friction between the mold and the punch, as well as a loss of the press force.

When measuring the electrical resistance of the resulting strontium lanthanum ferromolybdate target, high values of $R \sim 0.8 \cdot 10^3$ Ohm at T=300 K were established, which is most likely due to the high target density, which complicates the process of oxygen desorption due to kinetic limitations. As a result, the oxygen content in SLFMO is high and the oxygen index value corresponds to $\delta \sim 0$, which reduces the degree of ordering of Fe/Mo cations and lowers the density of electronic states at the Fermi level, weakening the severity of the ferrimagnetic and metallic properties of double perovskites. In this case, at room temperature, the concentration and degree of polarization of electrons in the conduction band decreases, which leads to an increase in electrical resistance. This leads to excessive charge accumulation on the target surface, causing fluctuations in ion plasma parameters and making it difficult to control the film deposition process, which in turn reduces the reproducibility of their physicochemical characteristics. The presence of bound oxygen in the target structure also has a negative effect, since heating its surface during sputtering leads to the release of oxygen from the target, which can disrupt the parameters of the ion plasma and increase the oxygen content in the films.

To ensure the possibility of annealing under conditions of control over the processes of SLFMO oxygen sorption-desorption, as well as increasing the cationic Fe^{3+} and Mo^{5+} ordering and, accordingly, improving the reproducibility of their physical characteristics, annealing of double perovskites was carried out using thermal cycling. Considering that the equilibrium values of the partial pressures of oxygen $pO_2 = 10^{-12}$ Pa at 1200 K and $pO_2 = 10^{-5}$ Pa at 1510 K, we used a thermal cycling mode of changing the temperature according to the mode 1470→1200→1470 K. In this case, lowering the temperature to 1200 K we obtain low values of $pO_2 = 10^{-12}$ Pa, at which the surface of the samples becomes depleted of oxygen. Subsequent heating of the sample to a temperature of 1470 K promotes the diffusion mobility of oxygen vacancies and, as a consequence, the penetration of oxygen vacancies deep into the sample. The use of thermal cycling in a continuous flow of $5\%H_2/Ar$ for 3 hours led to a significant improvement in the galvanomagnetic characteristics of the compound and the appearance of X-ray reflections (011) and (013) (Fig. 1).

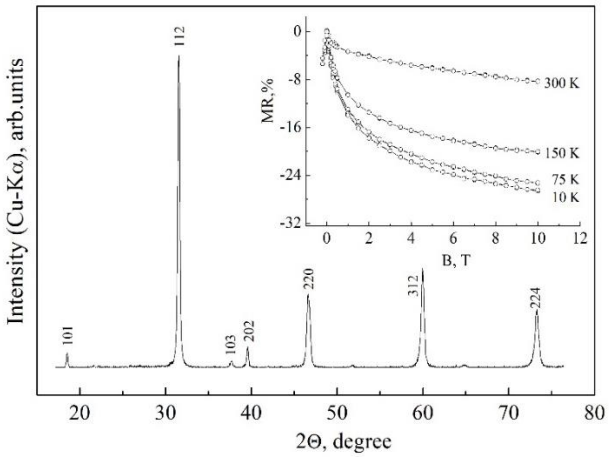

Fig. 1. XRD pattern of a high-density SLFMO sample annealed in a continuous flow of 5%H_2/Ar using thermal cycling. The inset shows the field dependence of the magnetoresistance of the resulting target.

According to X-ray phase analysis data, the superstructural ordering of Fe and Mo cations is P = 82 %. In this case, the magnetoresistance is 26.45% at T = 10 K, B = 10 T.

The authors are grateful for the support of this research within the framework of the Belarusian Republican Foundation for Fundamental Research projects No. F23ME-025 and No. F24MN-009.

Investigation of the aggregation of fullerenes C_{60} in water/NMP mixtures by molecular dynamics simulation

Balt Batgerel[1], Munkhdalai Chagdarjav[1], Narmandakh Jargalan[2]

[1]*Institute of Mathematics and Digital Technology, Mongolian Academy of Sciences, Mongolia*
[2]*Institute of Physics and Technology, Mongolian Academy of Sciences, Mongolia*

Email: jargalann@mas.ac.mn

Fullerenes, such as C_{60}, have attracted considerable attention due to their unique properties and potential applications in various fields. One area of interest is their behavior when dispersed in water/NMP (N-Methyl-2-pyrrolidone) mixtures. Understanding the aggregation of fullerenes in these mixtures is crucial for designing and optimizing processes involving fullerenes, such as drug delivery systems. In this study, we investigate the aggregation of fullerene C_{60} in water/NMP mixtures using molecular dynamics simulations. By simulating the motion and interaction of C_{60} molecules in different water/NMP ratios, we aim to elucidate the factors influencing their aggregation behavior. The results of the simulations show that the aggregation behavior of fullerene C_{60} in water/NMP mixtures depends on the ratio of the two solvents.

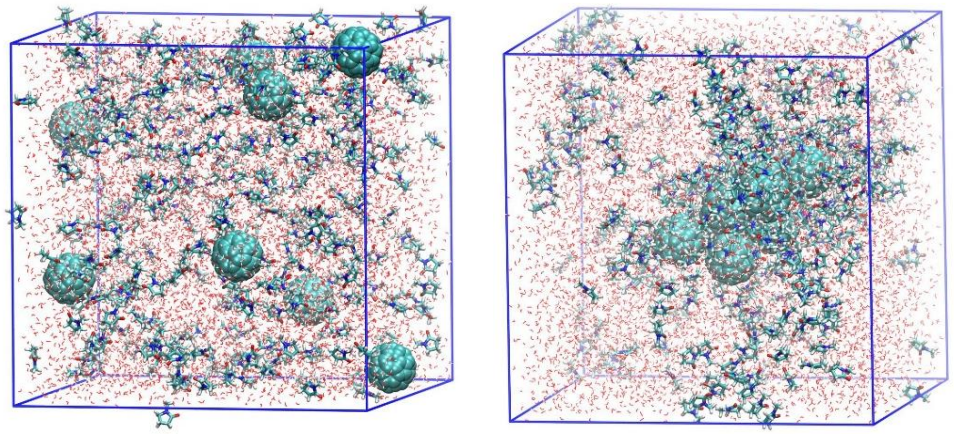

a) *b)*

Figure 1. Systems of C_{60} in water/NMP: a) initial state b) final state of simulation

In addition, the simulations suggest that the presence of NMP molecules plays a role in stabilizing the aggregates by surrounding the fullerenes. These findings provide valuable insights into the behavior of fullerenes in

water/NMP mixtures and can inform the development of strategies to control their aggregation for desired applications.

Keywords: fullerenes, aggregation, molecular dynamics simulation.

Supercontinuum generation from thin plates

Munkhbayar Gombosuren[1], Unurbileg Darmaa[1], Tsendsuren Khurelbaatar[2,3], Tuvjargal Norovsambuu[1], Davaasambuu Jav[1,4],

[1]*Laser Research Center, School of Arts and Sciences, National University of Mongolia, Ulaanbaatar 14201, Mongolia*
[2]*Center for Attosecond Science and Technology, Department of Physics, Pohang University of Science and Technology, Pohang, Gyeongbuk 37673, Korea*
[3]*Max Planck POSTECH/KOREA Research Initiative, Pohang, Gyeongbuk 37673, Korea*
[3]*Institute of Physics and Technology, Mongolian Academy of Sciences, Ulaanbaatar 13330, Mongolia*

The study of ultrafast events in nature, such as chemical reactions and charge transfer processes, requires the use of ultrashort light pulses to capture phenomena occurring on the femtosecond to attosecond timescales [1]. Various experimental methods have been developed to generate these pulses, including supercontinuum generation in gas-filled hollow-core fibers [2] and thin plates [3,4]. Thin plate supercontinuum generaion is particularly promising due to its simplicity and compact design. Previous studies have demonstrated single-cycle pulse generation using silicon dioxide (SiO_2) plates and multiple plate arrangements [5]. In this work, we theoretically investigate supercontinuum generation using a thin lithium fluoride (LiF) plate and compare it with SiO_2. Our simulations are based on the parameters of Laser Research Center amplifier system at the National University of Mongolia and aiming to identify the optimal conditions for generating ultrashort pulses with this setup.

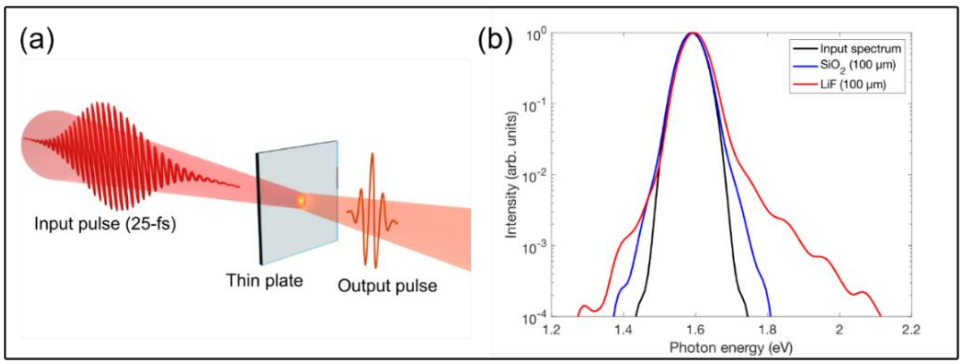

Figure 1. (a) Simplified scheme for thin plate supercontinuum generation method. (b) Simulation results.

In Fig. 1(b), we present the simulation results for supercontinuum generation using SiO_2 and LiF plates. We employed 0.5 mJ, 25-fs, 800 nm

laser pulses as the input (black spectrum in Fig. 1(b)), which were focused by a 100 cm focal length lens onto a thin plate with a thickness of 100 μm. The simulation conditions were kept consistent for both types of thin plates. For the SiO2 plate, the spectral broadening observed was relatively modest (blue spectrum in Fig. 1(b)). In contrast, the LiF thin plate exhibited significant spectral broadening. Therefore, LiF is more suitable and promising for achieving maximal spectral broadening with a minimal number of thin plates.

References

[1] F. Krausz and M. Ivanov, *Attosecond Physics*, Rev. Mod. Phys. **81**, 163 (2009).

[2] M. Nisoli, S. D. Silvestri, O. Svelto, R. Szipöcs, K. Ferencz, C. Spielmann, S. Sartania, and F. Krausz, *Compression of High-Energy Laser Pulses below 5 Fs*, Opt. Lett. **22**, 522 (1997).

[3] C.-H. Lu, Y.-J. Tsou, H.-Y. Chen, B.-H. Chen, Y.-C. Cheng, S.-D. Yang, M.-C. Chen, C.-C. Hsu, and A. H. Kung, *Generation of Intense Supercontinuum in Condensed Media*, Optica **1**, 400 (2014).

[4] A. Dubietis, G. Tamošauskas, R. Šuminas, V. Jukna, and A. Couairon, *Ultrafast Supercontinuum Generation in Bulk Condensed Media (Invited Review)*, arXiv:1706.04356.

[5] M. Seo, K. Tsendsuren, S. Mitra, M. Kling, and D. Kim, *High-Contrast, Intense Single-Cycle Pulses from an All Thin-Solid-Plate Setup*, Opt. Lett. **45**, 367 (2020).

Lignocellulose Composition of Preparation of Porous C arbon Materials and CO_2 Adsorption Performance R esearch

Wurentuya Bhnar [1], Ren Wu[1], Agula Bao[1]*

[1] *Inner Mongolia Key Laboratory of Green Catalysis, College of Chemistry and Environmental Science, Inner Mongolia Normal University, Hohhot 010022, Inner Mongolia, China*

*Email: agl@imnu.edu.cn

As the concentration of CO_2 in the atmosphere continues to increase, the environmental changes and climate disasters brought about by its greenhouse effect threaten the survival and long-term development of human beings [1]. As one of the major greenhouse gases, the development of carbon dioxide (CO_2) capture and storage technologies is currently a significant concern. Porous carbon materials are one of the effective methods for CO_2 capture and sequestration due to their excellent stability, adjustable pore size, diverse pore structures and environmental friendliness [2-3]. In order to realis their applications, there is an urgent need to find cost-effective raw materials for the preparation of porous carbon materials. In this paper, porous carbon materials were successfully prepared by using lignocellulosic composition as a carbon source and mild Kac as an adsorbent. According to the N_2 adsorption-desorption isotherm, it can be observed that the material shows a type IV adsorption-desorption trend [4]. In addition, the pore size distribution graphs showed that a large number of micropores and certain mesopores existed in the prepared materials, which had a positive effect on the adsorption of CO_2 [5]. In the CO_2 adsorption performance test, LCH-1 showed excellent CO_2 adsorption performance and stability among all the samples. The microporosity of LCH-1 was as high as 84.48%, and the CO_2 adsorption at 273 K and 298 K, 1 bar were 4.94 mmol/g and 3.31 mmol/g.

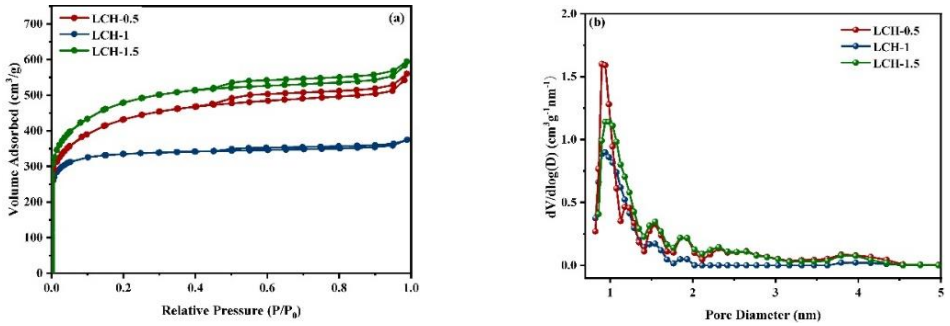

Fig. 1. (a) Nitrogen adsorption−desorption isotherms and (b) pore size distributions of sample

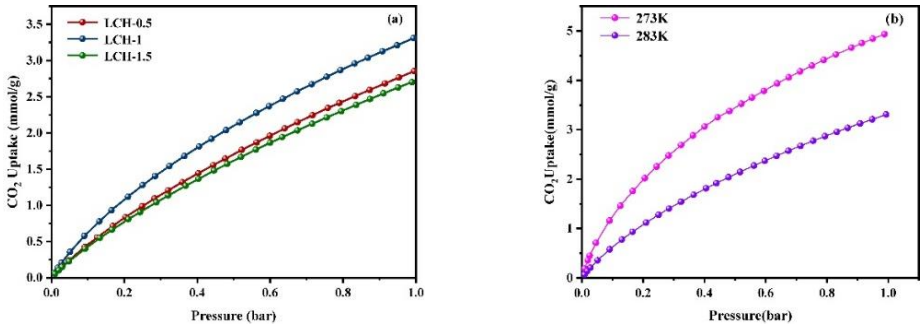

Fig. 2. (a) CO_2 capture capacity of the sample at 298 K and (b) LCH-1 adsorption isotherms at 273 K and 298 K

References

[1] W.P. Kong, J. Liu. Nitrogen-decorated, porous carbons derived from waste cow manure as efficient catalysts for the selective capture and conversion of CO_2, RSC Adv.9(2019).

[2] S. Park, S.M. Choi, S.H. Park. Nitrogen-doped nanoporous carbons derived from lignin for high CO_2 capacity, Carbon Lett. 29(2019).

[3] R. Wu, A Bao. Preparation of cellulose carbon material from cow dung and its CO_2 adsorption performance, J.CO_2 Util. 2023(68).

[4] Q. Li, S. Liu, L. Wang, et al. Efficient nitrogen doped porous carbonaceous CO_2 adsorbents based on lotus leaf, J. Environ. Sci. 103(2021) 268-278.

[5] N.P. Wickramaratne, M. Jaroniec. Importance of small micropores in CO_2 capture by phenolic resin-based activated carbon spheres, J. Mater. Chem. A. 1(2013) 112-116.

Preparation and characterisation of urea-modified lignin-derived porous carbon materials and their CO_2 adsorption properties

Bao Siriguleng[1], Gong Lingzhen[1], Bao Agula[1*]

[1]*Inner Mongolia Key Laboratory of Green Catalysis, College of Chemistry and Environmental Science, Inner Mongolia Normal University, Hohhot 010022, Inner Mongolia, China*

*Email: agl@imnu.edu.cn

Current carbon emissions originate mainly from fossil energy utilisation processes. About 95 per cent of industrial lignosulfonates are discarded or used as low-value fuels to meet energy needs [1]. Present study activated carbon was precarbonised and chemically activated to prepare activated charcoal from different lignins, and their adsorption properties had been investigated. The influences of carbon source selection with urea modification on the CO_2 adsorption performance of the materials were investigated. The selectivity, warmth of adsorption and cyclic steadiness of the materials had been in addition tested. The urea-modified porous carbon materials were prepared using dealkylated lignin (LCC), calcium lignosulfonate (CLS) and sodium lignosulfonate (SLS) as carbon precursors, KOH as activator and urea as nitrogen dopant. The CO_2 adsorption values of LCC-0.5N samples at 1 bar, 273 K and 298 K were 5.52 mmol/g and 3.90 mmol/g, respectively.

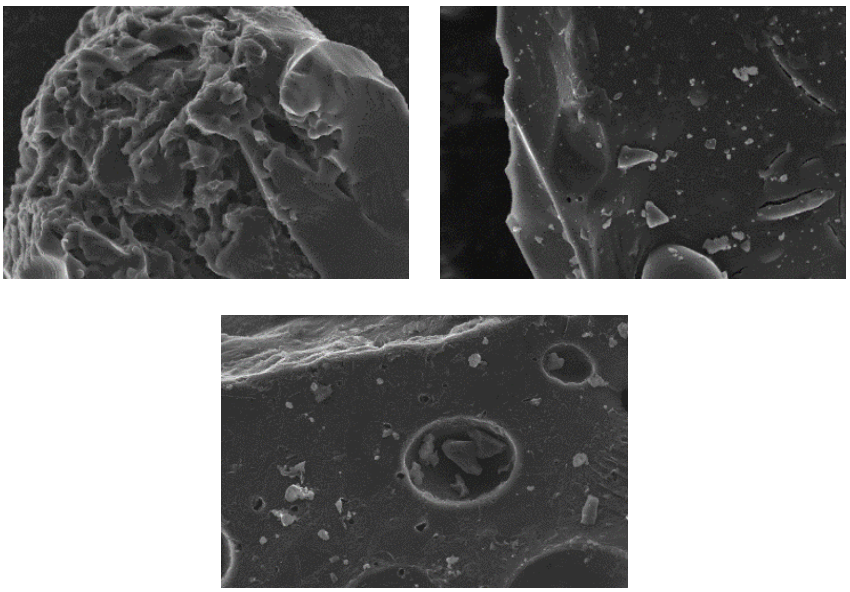

Fig. 1. SEM maps of LCC-0.5N (a), SLS-0.5N (b) and CLS-0.5N (c)

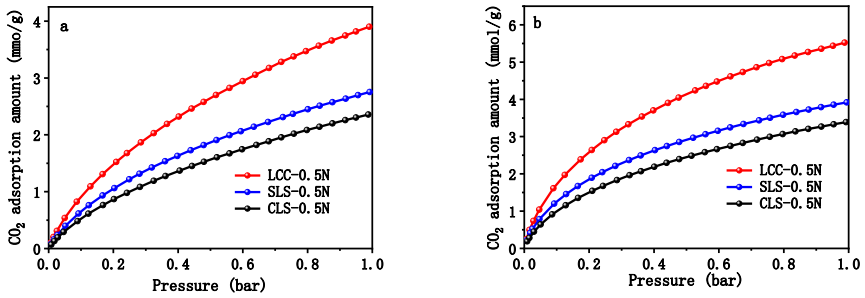

Fig. 2. CO_2 adsorption curves of X-0.5N at 1 bar (a) 298K and (b) 273K

References

[1] D.Kai, M.J.Tan, P.L.Chee, et al. Towards lignin-based functional ma terials in a sustai Green Chemistry, 2016, 18(5): 1175-1200.

Experimental studies of structural and optical properties of Nd-doped $LiYF_4$ compounds

Deng Lili[1], N.Tuvjargal[1,2*], N.Tsogbadrakh[1**] and J.Davaasambuu[2,3]

[1]*Department of Physics, National University of Mongolia, Ulaanbaatar 1420 1, Mongolia*
[2]*Laser research center, National University of Mongolia, Ulaanbaatar 14201, Mongolia*
[3]*Institute of Physics and Technology, Mongolian Academy of Sciences, Ulaan baatar 13330, Mongolia*

*Email: Tuvjargal@num.edu.mn
**Email: Tsogbadrakh@num.edu.mn

Herein, the $LiYF_4$ and Nd doped $LiYF_4$ compounds that are doped with rare-earth Nd^{3+} ions are synthesized by environmentally friendly technique and solid-state reaction method. The results of optical characterization of the Nd doped $LiYF_4$ compound are demonstrated. The outcomes of XRD, optical absorption and emission measurements show that doped sample is successfully synthesized. Optical absorption and emission results of Nd doped $LiYF_4$ compound obtain that this material cannot emit radiation with a several wavelengths in visible ranges. We have predicted and compared the structural parameters, electronic structure and absorption spectrum of the $LiYF_4$ and Nd doped $LiYF_4$ compounds using the random phase approximation (RPA) within the framework of density functional theory.

Keywords: visible laser, solid state reaction, optical absorption and emission, Visible laser, solid state reaction, DFT and RPA

Acknowledgements

This work is supported by the ShuSS-2020/61 project of fundamental research for Mongolian Foundation of Science and Technology in Mongolia. NT would like to acknowledge support from the ICTP through the Associates Programme for 2022-2024.

Preparation and Characterization of Carbon Aerogel by Freeze-drying Method

Jiayu Li[1], Tana Bao[1, 2], Altan Bolag[1, 2], Narengerile[1, 2], Yin Gang[1] and O. Tegus[1, 2]

[1]College of Physics and Electronic Information, Inner Mongolia Normal University, Hohhot, 010022, China
[2]Inner Mongolia Key Laboratory for Physics and Chemistry of Functional Materials, Inner Mongolia Normal University, Hohhot, 010022, China

Email: tanaph@imnu.edu.cn

Carbon aerogel is a kind of low-density solid with excellent properties such as high specific surface area, high porosity, and good conductivity. Carbon aerogel has a wide range of application prospects in the fields of thermal insulation and catalyst support. The use of abundant and low-cost non-toxic biomass resources as raw materials to prepare carbon aerogel can effectively reduce costs. In this paper, carbon gel was prepared by sol-gel method, and then carbon aerogel was prepared by freeze-drying method. The crystal structure was analyzed by Xray diffraction (XRD), the micromorphology was characterized by Scanning Electron Microscopy (SEM), the pore size distribution of the sample was analyzed by Barrett-JoynerHalenda (BJH) algorithm, and the surface area was compared by Brunauer-Emmett-Teller (BET) method. The experimental results show that the carbon aerogel is amorphous, forming a micro spatial network pore structure, and its pore size is mainly distributed in the range of 2-50 nm. The N_2 adsorption-desorption curve of the sample showed that a typical hysteresis ring was formed, and the adsorption amount of N_2 in the ring was very high, and the calculated specific surface area reached 367.5m^2/g, indicating that the carbon aerogel was a kind of gel skeleton mesoporous material with good strength and toughness.

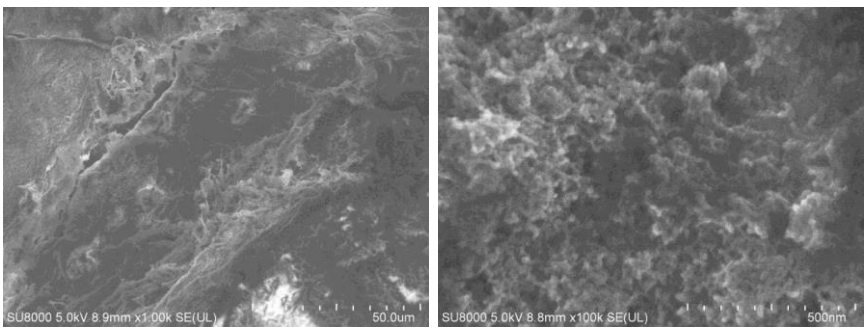

Fig. 1. SEM image of carbon aerogel

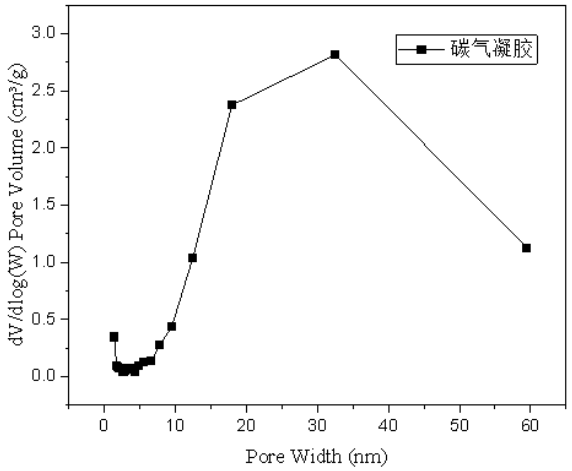

Fig. 2. BJH pore size profile of carbon aerogel

References

[1] J. Wang, M. J. Han, Y. N. Liu, et al. Multifunctional Microwave Absorption Materials of Multiscale Cobalt Sulfide/Diatoms Co-doped Carbon Aerogel [J]. Journal of Colloid and Interface Science, 646 (2023) 970-979.

[2] M. N. Zhen, F. Liu, C. Li, et al. Advances in Carbon Aerogels and Their Composites for Environmental Applications[J]. Materials China, 42(2023) 64-73.

[3] T. T. Zeng. Preparation and Application Properties of Carbon Aerogel Based Composites[D]. Dalian Polytechnic University, 2023.

Funding: This research was funded by the Natural Science Foundation of Inner Mongolia (Grant No. 2021MS05047 and 2021MS02025) and Fundamental Research Funds for the Inner Mongolia Normal University (Grant No. 2023JBQN041 and 2023JBBJ006).

Synthesis of luminescent matrix materials of rare earth Tb and Eu and its basic application in OLED devices

Anqi Wang[1], Gerile Naren[1,2,3*], LiangJun Wu[1], FangYi Xu[1,2,3*], Wei Wei[1,2,3*]

[1] *College of Physics and Electronic Information, Inner Mongolia Normal University, Hohhot 010022, China;*
[2] *Inner Mongolia Key Laboratory for Physics and Chemistry of Functional Materials, Inner Mongolia Normal University, Hohhot 010022, China*
[3] *Inner Mongolia Engineering Research Center for Rare Earth Functional and New Energy Storage Materials, Hohhot 010022, China*

Email: argl0622@163.com; naren0501@163.com

The low molecular weight rare earth organic complexes formed by the combination of rare earth metal ions and amino acids have excellent physical and chemical functional properties, which have attracted widespread attention from scholars at home and abroad. In this project, amino acid ligand compounds that have been developed by the guidance teacher's research group will be used to develop rare earth amino acid complex luminescent matrix materials through solution chemical reactions. The light absorption and fluorescence properties of these rare earth organic complex materials will be studied to obtain the best functional properties of rare earth organic complexes. Subsequently, we plan to design and develop small single-layer or double-layer OLED devices and organic solar cell devices and conduct photoelectric performance tests on the above devices.

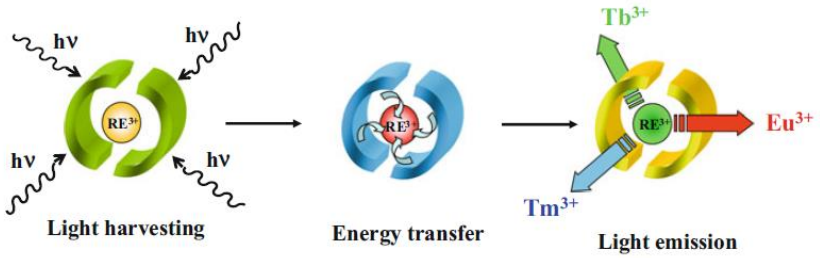

Fig. 1. Schematic diagram of organic ligand sensitized rare earth luminescence process.

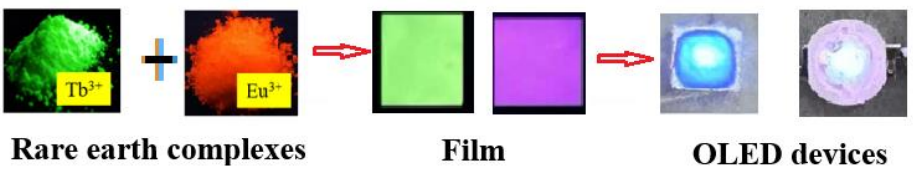

Fig.2. Rare earth organic complexes OLED optoelectronic devices

Acknowledgements: This project is supported by the Research Program of Science and Technology at Universities of Inner Mongolia Autonomous Region (Grant Nos. NJZZ23020); and Natural Science Fund Project of Inner Mongolia (Grant Nos. 2023MS02015); and Task Book for College Student Innovation and Entrepreneurship Training Program Project of Inner Mongolia (Grant Nos. S202310135038).

References

[1] Ying Z, Gerile N, Tana B, et al. Synthesis, Characterization, and DFT studies of Praseodymium (III) Octanoyl-DL-aminocarboxylate Complexes [J]. ChemistrySelect, 2022, 7(6): 1-11.

[2] Naren G, Bao T, Ning J, et al. Optical properties and aggregation behavior of environmentally friendly Lanthanum (III) acyl–alaninnate complexes[J]. Arabian Journal of Chemistry, 2020,13(6): 5864-5877.

Study on the structural and photophysical properties of N-acyl amino acid europium complexes

Gerile Naren[1,2,3*], Zihao Qiu[1], Aorigele Bohnuud[1], Rui Meng[1], Tana Bao[2,3]

[1] *College of Physics and Electronic Information, Inner Mongolia Normal University, Hohhot 010022, China;*
[2] *Inner Mongolia Key Laboratory for Physics and Chemistry of Functional Materials, Inner Mongolia Normal University, Hohhot 010022, China*
[3] *Inner Mongolia Engineering Research Center for Rare Earth Functional and New Energy Storage Materials, Hohhot 010022, China*

Email: argl0622@163.com; naren0501@163.com

In this paper, a series of acyl amino acid europium complexes were synthesized using N-acyl amido alanine as ligands, and their structures and photophysical properties were studied. The structural and functional group information of europium complexes was obtained by elemental analysis, as well as infrared and hydrogen nuclear magnetic spectral analysis (^{1}H NMR). The theoretical structure of the complexes was obtained by density functional theory (DFT) calculations; the theoretical structure of the complex was shown to be reliable by the comparison of theoretical and experimental vibrational and ^{1}H NMR spectra. Additionally, the photophysical properties of the solid complexes at room temperature were determined by analysis of UV-visible absorption and luminescence spectra. Moreover, the solvent effect on the luminescence performance of the complexes was investigated by testing the luminescence spectrum of the complexes in a methanol solution. Finally, the variable temperature spectral analysis provided information on the temperature-dependent variation of the luminescence properties of the complexes.

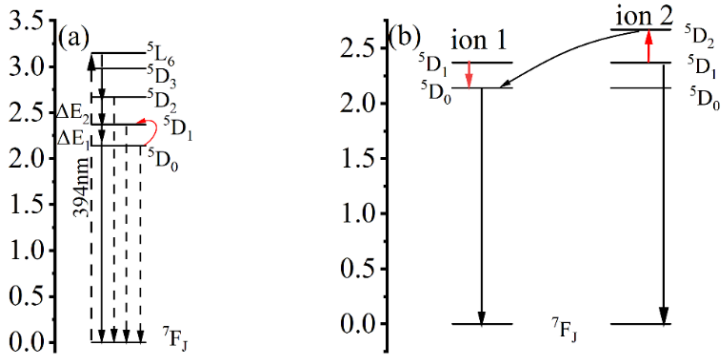

Fig. 1. (a) Variable temperature energy transfer diagram of the Eu^{3+}complex; (b) Schematic diagram of Eu^{3+}cross relaxation

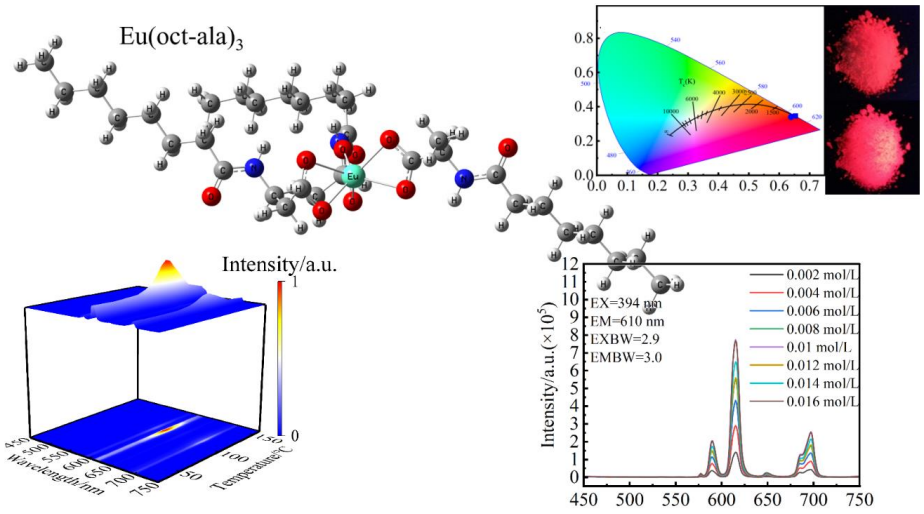

Fig.2. Molecular structure and luminescence of europium complexes

Acknowledgements: This project is supported by the Research Program of Science and Technology at Universities of Inner Mongolia Autonomous Region (Grant Nos. NJZZ23020); and Natural Science Fund Project of Inner Mongolia (Grant Nos. 2023MS02015).

References:

[1] Zhang J K, Gerile N, Zhang Y, Bolag A. Synthesis and luminescence properties of rare earth (Eu, Tb) complexes of octanoylphenylalanine. Solid State Phenomena. 2020; 310:22-8.

[2] Zhang H, Fan R, Chen W, et al. Two new dysprosium–organic frameworks contaning rigid dicarboxylate ligands: Synthesis and effect of solvents on the luminescent properties [J]. Journal of Luminescence, 2013, 143: 611-8.

Modeling of sound propagation in liquid medium depending on the size of air bubbles

B.B. Damdinov[1,2,*], A.I. Lyamkin[1], V.A. Prigozhikh[1]

[1] *Siberian Federal University, 79 Svobodny pr., Krasnoyarsk, 660041, Russia*
[2] *Institute of Physical Material Science of SD of the RAS, 6 Sakhyanova Str., Ulan-Ude 670047, Russia*

This paper presents a visualization of a well-known and important for practical applications problem of sound propagation in a liquid medium with bubbles. The model was studied by numerical modeling methods using COMSOL Multiphysics. A number of calculations were performed to produce visualizations based on the calculated acoustic and sound pressure distributions in the aquatic environment and on surfaces at different sound frequencies. The model allowed the observation of zones of increased and decreased acoustic pressure on the surface of air bubbles. In the future, the obtained results on the propagation of sound waves in a model water medium with bubbles will be used in the planned series of studies on sound propagation in a medium containing spherical nanoparticles of different nature.

Keywords: acoustic pressure, sound pressure, sound propagation, liquid media, gaseous inclusions, mathematical modeling, numerical methods

Determination of Thermal Conductivity of Silica Dioxide Tarcosil T-50 Nanopowder by Laser Flash Technique

Lygdenov Valery[1], Bardakhanov Sergei[2], Nomoev Andrey[1], Syzrantsev Vyacheslav[2]

[1]Institute of Physical Materials Science SB RAS, Ulan-Ude, Russia
[2]Institute of Theoretical and Applied Mechanics named after. S. A. Khristianovich SB RAS, Novosibirsk, Russia

Email: Lygdenov65@mail.ru

Nanopowders have good thermal insulation properties. Nanopowders of silicon dioxide have a meager thermal conductivity value, about 7×10^{-3} W/(m·K). The task of measuring the thermal conductivity coefficient of the above materials and other nanopowders is technically tricky.

One of the most accurate methods of measuring thermal conductivity can be considered the laser flash method. Using the example of the LFA 427 measuring device from Netzsch (Germany), its main advantages include performing measurements for a wide variety of materials and using a wide temperature range while in a very different gas environment or a vacuum with sufficient accuracy. To carry out the measurements, the nanopowder pressed in the form of a cylinder (12.6×2.5 mm) to a final density of 690 kg / m^3. This value is 6.3 times higher than the bulk density (110 kg/m^3).

Figure 1 shows the dependence of the thermal conductivity coefficient λ of the T-50 nanopowder sample in the compacted state on the temperature. It can be seen from the dependence that the coefficient of thermal conductivity depends on the measurement medium.

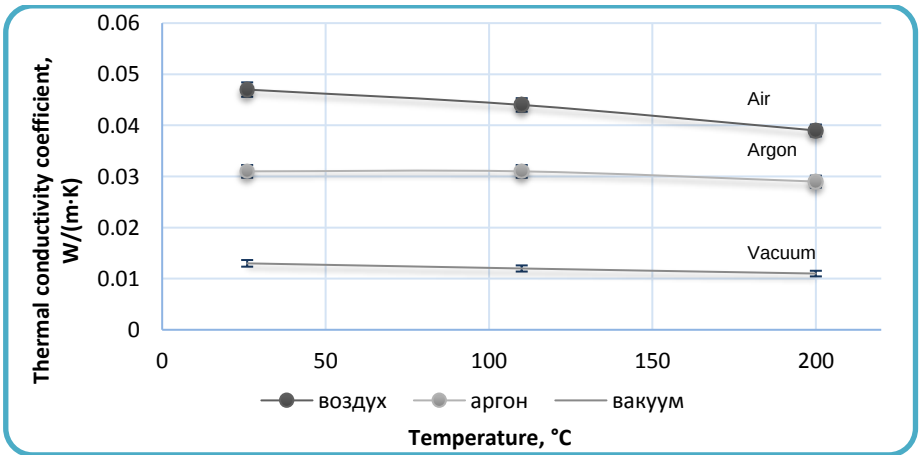

Figure 1. The dependence of the thermal conductivity coefficient of a sample of a compacted «Tarkosil» T- 50 nanoparticle on its temperature for three media.

The comparison shows that the thermal conductivity coefficient of the nanodispersed silicon dioxide powder «Tarkosil» T-50, even in the compacted state, has a lower thermal conductivity, which is almost 2-4 or more times lower than that of other heat-insulating materials of similar densities.

References

[1] A. V. Nomoev, S.P. Bardakhanov, V. V. Syzrantsev, and V.T. Lygdenov. Determination of thermal conductivity of silica dioxide Tarkosil T-50 nanopowder by laser flash technique // Journal of Engineering Thermophysics. 2016. № 2. vol. 25. pp. 174–181. (WoS).

Features of the formation of protective layers of chromium borides on the surface of die steels

Milonov A.S.[1], Mishigdorzhiyn U.L.[1], Lysykh S.A.[1], Semenov Yu.I.[2], and Kosachev M.Yu.[2]

[1]Institute of Physical Materials Science of the Siberian Branch of the Russian Academy of Sciences,
Sakhyanovoy Str. 6, 670047 Ulan-Ude, Russian Federation
[2]Budker Institute of Nuclear Physics of Siberian Branch Russian Academy of Sciences
Acad. Lavrentieva Pr. 11, 630090 Novosibirsk, Russian Federation

Email: terwer81@mail.ru

In this work, protective coatings based on chromium borides were formed to improve the performance properties of D2 die steel, obtained by electron beam synthesis of the Cr_2O_3-B-C reaction mixture and surfacing of self-propagating high-temperature synthesis (SHS) products on the steel surface. The experiments were carried out at the Institute of Nuclear Physics named after G.I. Budker SB RAS, Novosibirsk on an electron beam welding installation (ELS - V - 60/500). The beam diameter was 1.5 mm, the accelerating voltage was 50 kV, the pressure in the chamber was 4.6 * 10^{-3} Pa, the filament current was 18.5 mA. Processing time 12 seconds. The layers turned out to be about 300 microns thick. In Fig. 1 shows that the structure of the layer is heterogeneous; there are gray inclusions, which contain chromium carbides and borides.

Fig.1. CrB_2-based layer on D2 die steel.

The heterogeneity of the layers is explained by the fact that during the formation process the surface of the steel melts. Particles of SHS products during steel crystallization are located in a soft metal matrix, which

contributes to the formation of a layer with significantly reduced brittleness.

The results obtained give us the opportunity to consider the use of electron beam synthesis of SHS products and surfacing on the surface of tool die steels.

Acknowledgments. The work was carried out with financial support from the state assignment of the Ministry of Science and Higher Education of the Russian Federation, scientific topic No. 0270-2024-0010

Investigation of multifunctional diffusion layers created on the surface of iron-carbon alloys by combined methods of chemical-thermal treatment and electron beam treatment

Stepan Lysykh[1], Undrakh Mishigdorgiin[1], Alexandr Milonov[1], Vasilii Kornopoltsev[2]

[1]*Institute of Physical Materials Science of the Siberian Branch of the Russian Academy of Sciences, Ulan-Ude.*
[2]*Baikal Institute of Nature Management of the Siberian Branch of the Russian Academy of Sciences, Ulan-Ude.*

Email: lysyh.stepa@yandex.ru

An urgent task of modern materials science is to extend the life cycle of machine parts and tools by creating functionally gradient coatings and layers. In mechanical engineering, such methods of chemical and thermal treatment have been widely used: nitriding, boration, etc. Boration has many advantages over other methods, but also a number of disadvantages that prevent its widespread use. To solve these problems, it is proposed to carry out a method of chemical-thermal treatment- boromedification, with its further modification by an electron beam. The work carried out studies on the production of diffusion layers on 45 and 5nm steels by chemical and thermal treatment with subsequent modification of these layers by an electron beam. The results of studies of the structure of layers and microhardness are presented.

Fig. 1. Diffusion layer on 5khnm Steel: Left) after WHO. Right) WHO+EPO.

References

[1] Kharaev, Y.P.; Kornopoltsev, V.N.; Lysyh, S.A. Opredeleniye sostava smesi pri poverkhnostnom uprochnenii stali borom i med′yu [Identification of a mixture composition for surface hardening of steel with boron and copper].

Polzunovskiy Al'manakh 2016, 4, 142–144 https://elibrary.ru/item.asp?id=27711859 (In Russian)

[2] Krukovich, M.G.; Prusakov, B.A.; Sizov, I.G. Methods of Reducing the Brittleness of Boronized Layers: The Parameters of Boriding Technology Aimed at Determining the Plasticity of Boronized Layers. In *Plasticity of Boronized Layers*; Springer Series in Materials Science, Springer: Cham, Switerland, 2016; Volume 237, pp. 111–196. https://doi.org/10.1007/978-3-319-40012-9_8.

Reactive plastic materials modified by mechanically activated particles

Tatiana Grigorieva[1], Yauheni Auchynnikau[2], Yahenia Eysimont[2]

[1]*Institute of Solid State Chemistry and Mechanochemistry, Kutateladze , 18, Novosibirsk, 630090, Russia,*
[2]*Yanka Kupala State University of Grodno, Ozhesko 22, Grodno, 230021, Belarus*

Email: ovchin@grsu.by

Modern products and parts are currently made from a wide range of different composite materials, which can significantly change the performance characteristics of various types of machines and devices used in various types of production. Thus, solving the problem of creating base materials used as matrices for modification is one of the pressing problems of modern materials science that needs to be solved. However, there is another promising direction in the field of creating composite materials - the creation of new modifiers that make it possible to significantly change the modified materials, giving them the necessary physical, chemical, technical, etc. characteristics.

To create new types of modifiers, various types of technologies are used based on physical, chemical, physicochemical principles of production. In recent decades, to obtain modern modifiers used in the chemical industry, medicine, and mechanical engineering, the technology of mechanochemical synthesis has been used, which consists of the simultaneous occurrence of both a mechanical effect on the modified material and targeted chemical synthesis. As a result of the synergistic effect, materials are formed that are qualitatively different in properties from the starting materials involved in the synthesis of the modifier.

In the course of the work carried out, the morphology of mechanically activated particles was examined. According to the presented data on a composite material based on epoxy resin modified with nanodispersed mechanically activated particles of polyvinyl alcohol and polyvinyl buteral, they are characterized by a developed morphology. The morphology of the surface of polymer chips changes with changes in the resolution of shooting the chip surface.

The tribological characteristics of composite materials based on an epoxy matrix modified by mechanically activated particles of kaolinite-PVA, kaolinite-polyvinyl buteral particles have been studied. It has been shown that the cluster structure of mechanically activated particles of kaolinite-PVA, kaolinite-polyvinyl buteral, representing a combination of nano-sized elements of the polymer fraction and oligomeric products of

various masses, located on the surface of an ultra-small or nano-sized kaolinite particle allows the formation of transferred (separation) layers in the friction contact zone, synergistically combining the most favorable tribological characteristics for metal-polymer friction pairs.

Physical and mechanical characteristics of electrospark coatings

Y.Auchynnikau[1], V.Mikhailov[2], A..Svistun[1], D.Linnik[1], Y.Matuk[1], A.Auchynnikau[1]

[1] *Yanka Kupala State University of Grodno, Ozhesko 22, Grodno, 230021, Belarus*
[2]*Institute of Applied Physics, Chisinau, 5 Academiei str., Moldova*

Email: ovchin@grsu.by

Increasing the service life of machine parts and mechanisms is achieved by improving the structure of the material, as well as modifying the surface layers of products of various designs. One of the widely used methods for modifying the surface of various conductive materials is the method of electric spark alloying of metals. Electrospark alloying (ESA) of solid conductive surfaces consists in the fact that as a result of passage between the electrodes, a directed ejection of the electrode material occurs. In the process of electric spark discharge, predominantly the anode is destroyed. Since ESA is carried out in a gaseous environment, this leads to the fact that, under given conditions, the anode material, which is mainly in the gas or liquid phases, is deposited on the cathode. As a result of the interaction of the applied material with the cathode material and the environment, a layer with certain physical and mechanical characteristics is formed on the cathode. This layer has a complex chemical composition and structure and usually contains not only the anode material, but also solid solutions, chemical compounds, various alloys and pseudo-alloys. Using a method that combines low-voltage high-current pulses and an imposed strong electric field (0.5-3 kV/mm) in the interelectrode gap. The proposed approach has made it possible to significantly expand the range of materials used (metals, semiconductors, dielectrics). It is possible to assume the following process of coating formation using this methodological approach: powder particles entering the interelectrode working gap cause an increase in the electric field strength to a value greater than the dielectric strength of the gap, as a result of which a discharge of the capacitance of the spark generator is initiated. Under the influence of the energy released in the spark discharge channel, a solid powder particle, depending on the discharge parameters, the mass of the particle itself and its thermophysical properties, partially or completely transforms into a liquid or vapor phase and is applied to the surface being treated. Due to the short-circuiting of the spark gap discharge channel, the voltage of the constant electric field drops almost to zero, and then, after deionization of the spark gap, it takes on its previous value, i.e. In a

certain volume, a pulsed change in the electric field occurs. The subsequent entry of a particle into the discharge channel area again causes a low-voltage high-current pulse. It should be noted that the entry of even one particle into the interelectrode gap, with a sufficient intensity of the electric field applied to the gap, leads to the initiation of a high-current discharge, which makes it possible to selectively influence an individual particle with high temperatures and shock waves that arise during a spark discharge.

High-voltage ignition of the working gap, which occurs when powder particles enter the interelectrode gap, contributes to the release of higher instantaneous thermal power in the discharge channel compared to a discharge without ignition. Thus, this technological approach is quite promising for the formation of electric spark coatings.

To determine the optimal mode in which the maximum amount of powder could fall into the discharge zone, the vibration frequency of the processing electrode was slowly varied from 100 to 30 Hz. Both industrial and experimental installations were used as sources of pulsed discharges. The ESA process was carried out in the range of discharge energy values from 0.3 to 10.0 J. In the course of the research, the change in the mass of the cathode of the modified material was studied when applying coatings from tungsten carbide powder.

It was found that at all values of the discharge energy, almost the same amount of material was deposited on the cathode, which does not fit into the well-known relationship $\gamma=f(E)$, in which it is established that the mass transfer of the anode to the cathode surface is directly proportional to the magnitude of the pulsed discharge energy. In our opinion, this result can have two explanations. The introduction of tungsten carbide powder into the gap during the ESA process significantly changes the mechanism of formation of the strengthened layer on the cathode. The anode no longer plays the primary role of delivering eroded material to the cathode surface. This role mainly belongs to the powder material. The introduction of tungsten carbide powder into the gap leads to a significant modification of the coating formation mechanism and indicates that the previously established criteria (thickness, deposition rate, etc.) are valid only for the case of a compact anode.

The morphology of TiAlC coatings formed using the proposed technology was studied using scanning electron microscopy. This class of coatings was obtained by sequentially processing steel 45 with titanium, aluminum and graphite electrodes in the electrode oscillation mode and changing the discharge energy value within the range (0.3÷3.0) J.

According to the data obtained, a coating with a morphology similar to “shagreen skin” is formed. Compared to coatings produced using standard

electrospark alloying technology, fewer defects and pores are observed in the formed coatings. Nanometer-sized structures are formed in the coatings under study, which may indicate nanostructuring processes in coatings obtained by combining low-voltage high-current pulses and an imposed strong electric field in the interelectrode gap. The work was carried out within the framework of the T22MLDG-004 project.

References

[1] Mihailov, V.Kazak, N., Ivashcu, S., Rukuiza, R., Zunda, A, Auchynnikau, Y. Synthesis of Multicomponent Coatings by Electrospark Alloying with Powder Materials / Coatings, 2023, 13(3), 651

[2] Auchynnikau, Y. Corrosion resistant electric spark coatings / Y. Auchynnikau // Modern scientific challenges and trends. Issue 4 (38), Part 2. – Warszawa: iScience, 2021. – С. 417-419.

[3] M. P. Seah, Adhesion-induced interface decohesion, Acta Metall., 28 (1980) 955 – 962.

[4] Gerkema and A. R. Miedema, Adhesion between solid metals: observations o f interfacial segregation, effects in metal film lubrication experiments, Surf. S ci., 124 (1983) 351.

High-entropy vacuum coatings

Nikolai Chekan[1], Igor Akula[1], Yauhenia Eisymont[2], Aleksei Auchynnikay[2]

[1]*Physical-Technical Institute of the National Academy of Sciences of Belarus Minsk, 10 Academician Kuprevich str. 220084, Belarus*

[`2] *Yanka Kupala State University of Grodno, Ozhesko 22, Grodno, 230021, Belarus*

Email: ovchin@grsu.by

Currently, there is a fairly large number of works devoted to the growth processes of coatings based on transition metal nitrides, in particular TiN, formed under various deposition regimes. Titanium nitride coatings formed on steel samples were studied. Studies of the surface of substrates carried out by atomic force microscopy indicate significant changes in the topography and morphology of titanium nitride after the deposition of oligomeric films. The formation of a base coating of titanium nitride was carried out using the method of reactive electric arc evaporation using a URMZ.279.048 installation. As a substrate, steel plates or rods (10 mm in diameter) made of steel 45, hardened to 58-60 HRC with a surface finish of Ra = 0.25 μm, were used. A team of researchers led by Joe Greene and Ivan Petrov studied the growth and formation of the microstructure of TiN, TiAlN and related compounds produced using various technological regimes. During the deposition of coatings, the energies of the incident ions on the surface of the metal substrate varied, and the bias voltage changed. This approach made it possible to provide an understanding of the role of ion energy and surface diffusion in the processes of formation of microstructures of these coatings [1-3]. AlSiN coatings using an AlSi source with a double cathode containing 12 at.% Si formed at 450°C were studied by a team of authors led by A.P. Laskovnev. The work showed that the hardness of the coatings was about 35 GPa, but the coatings had poor adhesion to the surface of the substrate. AlTiN coatings have high hardness, sufficient resistance to oxidation when exposed to high temperatures, resistance to fatigue failure, and are widely used to modify inserts made of superhard materials to increase the service life during cutting. However, with an increase in the feed speed of the cutter and the rotation of the workpiece itself, the traditional AlTiN coating does not achieve the expected increase in service life. One of the effective methods for increasing the wear resistance of AlTiN-based coatings is the introduction of Si into the composition of this chemical compound. According to the studies carried out, amorphous Si_xN_y is released at the AlTiN grain boundary, which can limit the growth of coating grains. At the same time, nanocomposite

structures are formed, which leads to improved mechanical properties and increased resistance to high-temperature oxidation. On the other hand, Si contained in AlTiSiN coatings delays the decomposition process of Ti–Al–N during annealing and, thus, allows maintaining high hardness values at elevated temperatures. As a result, AlTiSiN coatings have better thermal stability than AlTiN. However, this effect is accompanied by compaction of the coating structure and inevitably leads to an increase in residual compressive stresses in the coatings, which leads to a decrease in the impact resistance of the coatings and limits their use in severe operating conditions of the processing tool . A number of studies confirm that hardness has become one of the key factors affecting cutting performance. Increased wear resistance, low internal residual stresses, high hardness and adhesive interaction are the most promising directions in the development of surface engineering related to the creation of coatings for metalworking. In recent years, methods have been proposed to reduce residual internal stresses and improve the plasticity of hard and superhard coatings. Altin-based coatings are of interest as anti-friction coatings, because Nanocomposite phases have been identified in their structure, which influence the properties of these compounds. In some cases, they can replace lubricants and coatings based on molybdenum disulfide, graphite, and diamond-like coatings. Compositions of TiAlN + C coatings were proposed; this approach was supposed to provide a controlled change in hardness during friction, and this effect is associated with structural changes in the protective layers based on altin. The influence of carbon on the microstructure of thin films of the carbon influence series Ti, Al)(N, C) with different carbon contents (0–28 at.%) was determined, which were formed by reactive magnetron sputtering of a TiAl target in a mixture of Ar, N_2 and CH_4. Elemental composition (Ti, Al)(N, C) coatings were determined by micro-X-ray spectral analysis with an accuracy of 1–2% for carbon as the main element of the coatings. According to optical and scanning electron microscopy data, a fairly large number of globular formations are formed in the structure of the coatings, the size and concentration of which depends on the technology of formation and the chemical composition of the coatings. . As a result of deposition of coating material in a vacuum using an ion-plasma flow, nanophase objects are formed in the coating structure, which should lead to significant changes in the strength and adhesion characteristics of the deposited layers. In AlTiSi (C,N) coatings, a large number of inclusions are observed that are in the micron range in size. These formations are agglomerates of lower-sized particles. Perhaps these particles are phases of three-component or more compounds, like MAX phases.

References

[1] Auchynnikau Y. et al. Adhesive activity AITiN layers based on forming polymer coatings // The proceedings of the Austrian-Slovenian Polymer Meeting 2013 [Elektronski vir] / Austrian-Slovenian Polymer Meeting-ASPM 2013, 3-5 April 2013, Bled, Slovenia; editors Majda Žigon, Teja Rajšp.- El. zbornik. - Ljubljana: Centre of Excellence PoliMaT, 2013. – P. 256- 257.

[2] Auchynnikau Y. Tribotechnical Characteristics of Composite Coatings Based on Zirconium Cabonitride Subjected to Cryogenic Treatment/ Y. Auchynnikau [et al.] // Materials Science. Non-Equilibrium Phase Iransformations. International Scientific Jurnal.- 2018 .- T.IV. - № 4.- C.118-121.

[3] Auchynnikau,Y.V. Tribotechnical characteristics of comopsite cjatings base d on zirconium carbonitride subjected cryogenic treatment / Y.V.Auchynni kau [and etc.] // International sientific journal " Material science" -2018 - №4 - P.118-121.

Graphene-containing polymer materials

Alexandr Voznyakovsky[1], Alexey Voznyakovsky[1], Yauheni Auchynnikau[2], Yauhenia Eisymont[2]

[1]*The Ioffe Institute, Politekhnicheskaya , 126, St. Petersburg, 194021, Russia*
[2] *Yanka Kupala State University of Grodno, Ozhesko 22, Grodno, 230021, Belarus*

Email: ovchin@grsu.by

Today, nanotechnology is used in various fields of science, engineering and technology, such as automotive, aerospace and military, dentistry, medicine and electronics. Nanocomposites are matrix materials containing more than one component, in which any of them can be in the nanorange. The use of nanomaterials can improve productivity in the manufacture of composites and overcome technological limitations in the processing of traditional polymer materials. Production of polypropylene and polyethylene reached 177.5 million tons in 2015, indicating a high global demand for these materials in products and structures for a variety of applications. This is due to the fairly low cost of polyolefins, good mechanical and physical properties, which are used in a wide variety of fields. Raw polymers without any additives may not meet the requirements of everyday life. The increase in demand for polymers is achieved by improving parameters such as hardness, elasticity, wear resistance, which can be achieved by adding some additives and creating composites that meet today's needs. Recent trends in polymer preparation play an important role in the use of nanofillers and nanofibers for the production of nanocomposites. Adding a modifier to any polymer material improves the interfacial interactions of inorganic and organic modifiers with polyolefin chains when preparing nanocomposites. During the modification process, various supramolecular systems are created with morphological characteristics significantly different from the original polymers, which affects the physical, chemical and thermophysical characteristics of polymer materials [1-3].

Polyethylene (PE) is one of the most widely used commercial polymers due to its good mechanical properties, chemical resistance and ease of processing. The use of nanofillers as polyethylene modifiers is an active area of research due to the dramatic change in the physical and mechanical characteristics of the modified material and specific properties. The term nanomodifier can be formulated as follows - a material that has geometric dimensions in at least one dimension that are in the nanometer range. The introduction of a nanofiller also affects the structural characteristics of polyethylene, since the physical properties of polymers

directly depend on the structure. The mechanical and physical properties of many polymer materials are determined by the habit of crystallites, which are responsible for the structure and morphology of polymers and compositions based on them.

The purpose of this work was to study the structure of composite materials based on polyolefins (PO) modified with nanodispersed graphene-like particles obtained using SHS technology. Low-density polyethylene (HDPE) grade 277-03 (GOST 16338-85) and high-density polyethylene (LDPE) grade 16207-020 (GOST 16337-85) were used as research objects. The polymers were modified with nanodispersed graphene-like particles obtained using SHS technology.

This modifier is obtained using the technology of self-propagating high-temperature synthesis from organic raw materials in a mixture with special combustible materials and catalysts. The size of primary nanocrystals is in the range of 5-10 nm. The compositions were prepared by mechanically mixing the initial PO powders with filler. Samples for physical and mechanical tests were obtained by injection molding. The filler content in the composition varied from 0.01 to 1 wt%.

To determine structural changes in HDPE and LDPE upon the introduction of ultrafine clusters of synthetic carbon substances, X-ray patterns obtained on a general-purpose X-ray diffractometer DRON-3.0 were studied.

In the X-ray diffraction patterns of HDPE and LDPE modified with ultradisperse clusters of synthetic carbon in the region of diffraction angles 2θ = 15-29^o (for HDPE) and 2θ = 11-32^o (for LDPE), a distinct halo is observed with quite pronounced Bragg maxima superimposed on it. In the area of angles 2θ=36-47^o (for HDPE) and 2θ=32-47^o (for LDPE), a second, more blurred halo is noted on the X-ray images.

The calculation of the degree of crystallinity showed that the introduction of the modifier does not change the degree of crystallinity of the modified polymers. The degree of crystallinity does not depend on the concentration of the modifier and remains constant and is ~ 94%.

However, the modifier affects the average size of polyethylene crystallites. The introduction of 0.01% modifier into HDPE leads to a decrease in crystallite size from 358 to 350. Further increase in graphene content reduces the average crystal size to 308 (0.5% concentration). A similar dependence of the sizes of crystalline aggregates of polyolefins on the concentrations of nanodispersed graphene particles is also typical for LDPE.

References.

[1] Auchynnikau, Y. Operational characteristics of nanocomposite lubricants / Y. Auchynnikau // Machines. Technologies. Materials. – 2021. – Т. XV. – № 8. – С. 325-327.

[2] Auchynnikau, Y. Composite polymeric materials modified by nanodispersion functionalized particles/ Y. Auchynnikau, A. Voznyakovskii, A. Voznyakovskii // Machines. Technologies. Materials. 2019.- № 10.- С.471-473.

[3] Vozniakovskii, A., Voznyakovskii, A., Kidalov, S., Ovchinnikov, E., Kalashnikova, E. Thermal conductivity and heat capacity of nanofluid based on water modified by hybrid material of composition detonation nanodiamonds- carbon nanotubes Fullerenes Nanotubes and Carbon Nanostructures 30(1), c. 5-9, 2022.

Thermogravimetric and BET analysis on discharge products

J.Vanchinkhuu[a], M.I.Markevich[b], Ts.Erdenebat[c] , and G.Buyantsetseg[d]

[a] *Department of Physics, School of Arts and Sciences, National University of Mongolia, Ulaanbaatar, Mongolia*
[b] *Institute of Physics and Technology, National Academy of Sciences of Belarus, Minsk*
[b] *Laboratory of New Materials, School of Applied Science and Engineering, National University of Mongolia, Ulaanbaatar, Mongolia*
[d] *Analytical laboratory, Division of Material Science, Institute of Physics and Technology, Mongolian Academy of Science, Ulaanbaatar.*

We have considered the measurement results of the thermogravimetric (TG) and Brunauer-Emmett-Teller (BET) analysis of the carbon products from the DC arc of high current [1, 2] and the raw original graphite material. The TGA measurements was taken in nitrogen atmosphere at TGA21000 and the weight variation in percent on temperature was given in Fig 1. The similar study for carbon materials can be found in Ref. [3, 4]. The measurement results were processed on Mathematica software. The measurement data is of course a noisy and includes many of the same values at one values of temperature. In first step of data processing, the same values were changed to their mean values and at next step, the noisy data is filtered to the smooth data. The raw and smooth (filtered) data were depicted in Fig. 1 as the residue mass percentage versus temperature. Although the weight gain in plot is, in general, related to the chemical reactions leading to formation of compounds and the adsorption of gases on samples, the observed gain in the beginning of the plot is mainly caused by the buoyancy effect in which the density of surrounding gas decreases and does the lifting force. However, the gradual gain observed in the end part of the plot for the graphite is caused by newly arisen pores with high temperature and the adsorption of surrounding nitrogen on it because the samples' porosity the increases at high value of temperatures which result is given by the BET analysis. This gain was not observed for the product and it means the product became already porous material. The plots tell us that the samples have multistep decomposition upon heating. This says that the samples might have three different phases of decomposition. The comparing the medium step of decomposition for two samples shows that the decomposition temperature range clearly shifted each other and broaden for the product. The tendency TGA curves for two samples resembles but, the rates are different.

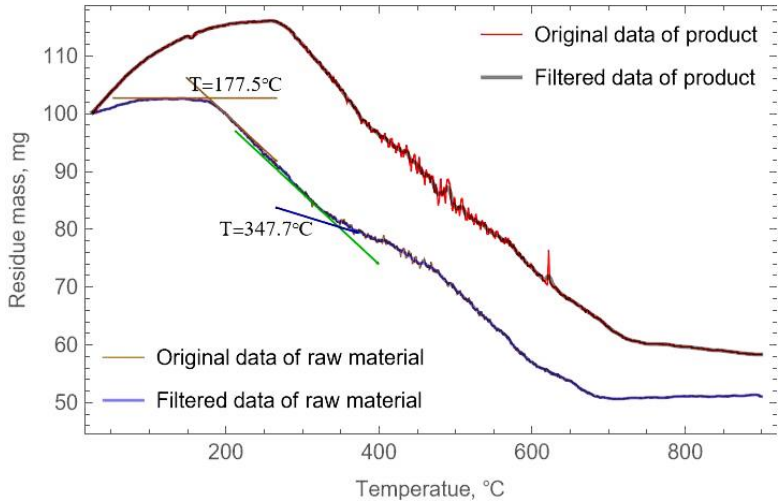

Also, the thermal stability, which is indicated by the initial disintegration temperature, is seen increased by the discharge processing. Temperatures of decomposition for each decomposition step can be determined by intersections of tangent lines. For simplicity and clearance of figures, we showed only four tangent lines and marked the corresponding temperatures. More accurate analysis on these samples can be done by using the derivative TG (DTG) analysis and this analysis reveal several high peaks in a temperature range of 400-550°C.

The BET analysis of the samples was done in Nitrogen gas at Quantchrome v5.21. The summary of overall measurement resultы related to surface and volume is shown in the Table 1. From the table, we can see that the pore volume and surface values determined in different way are almost the same with low difference range. The BET data indicates that the porosity graphite, which are related to absorption volume and surface, significantly increased by processing with discharge of increasing current. The results also, shows that the sample taken at the current of 90A has the highest value of porosity.

These means that one can improve the radio absorbing material of increased absorbing surface. The product, currently we have taken has the greatest absorbing surface area for absorption which is also valid for radio absorption [5]. The pore volume characteristics for samples of product confirms the observed results in TGA measurements. The data shows that most of pores in graphite are micro pores whereas it is mesopores in the products.

Table 1. Summary of the BET analysis results of porosity characteristics for samples

Porosity characteristics	Sample 1 (pure graphite)	Sample 2 (Product at I=50 A)	Sample 3 (Product at I=90 A)
Langmuir Surface Area: m^2/	NA	286200	NA
BJH method cumulative adsorption surface area, m^2/g	8688	21333	27650
DH method cumulative adsorption surface area, m^2/g	8961	21620	28280
t-method external surface area, m^2/g	12500	19970	26290
DFT cumulative surface area, m^2/g	11470	42790	20530
Total pore volume for pores with Radius less than 152737 Å at P/Po= 0993692, cc/g (cm^3/g)	158.9	671.8	590.20
BJH method cumulative adsorption pore volume, cc/g (cm^3/g)	157.8	671.8	590.0
DH method cumulative adsorption pore volume, cc/g (cm^3/g)	153.3	651.7	573.3
HK method micropore volume, cc/g (cm^3/g)	2.554	6.961	7.682
SF method micropore volume, cc/g (cm^3/g)	0.5864	0.4585	0.3726
DFT method cumulative pore volume, cc/g (cm^3/g)	111.5	435.9	49.74

References

[1] J.Vanchinkhuu, et al., "Structural Features of Products Formed during DC Arc Discharge in Water." Solid State Phenomena 288, 71–78, 2019.
[2] Vanchinkhuu et al., "Research Results of Discharge Products", Solid State Phenomena, Vol. 323, 113-118, 2021.
[3] A.Shahverdi et al., J Therm Anal Calorim, 110, 1079–1085, 2012.
[4] A.G. Bannov et al, Journal of Thermal Analysis and Calorimetry, 142, 349–370, 2020.
[5] R.Perez, et. al., Journal of Science: Advanced Materials and Devices 7(4),100454, 2022.

Chemical composition determination of black fingerprint powders

Kh.Tuvshin-Erdene

University of Internal Affairs, Mongolia

Email: tuvshin908@gmail.com

Knowing the chemical, physical, and morphological composition of these powders could prove significant in powder choice and print collection. EDS was used to identify the chemical composition and chemical ratios of each of the powders. This study characterizes five black fingerprint powders using energy dispersive X-ray spectroscopy (EDS) The following black fingerprint powders were analyzed: BVDA-1, Sirchie-1, Russia powder-2, Mongolia powder-1 /made in laboratory/. Each powder manufacture, name, and label are summarized.

Research on the seed peeling process on bull-dect equipment

Amartuvshin Oidov[1], Dovchinvanchig Maashaa[2*]

[1]*Department of Electrical Engineering and Electronic, School of Engineering and Technology, Mongolian University of Life Sciences, Ulaanbaatar, Mongolia*
[2] *Department of Physics and mathematics, Applied Sciences, Mongolian University of Life Sciences, Ulaanbaatar, Mongolia*

Email: dovchinvanchig@muls.edu.mn

We imagined a process to peel and seed by friction and stroke deformation action on rolling hub and compressing deck equipment and the mathematical model was processed. New modeled compressing deck is designated to create periodic and vibrational force on the seed within the limit of elasticity force. Friction force is created on the rolling hub equipment depending on the normal force to be determined on elasticity force created on seed and grain, the seed is peeled out as a result of periodic force created between rolling hub and compressing deck. When impact of normal force is within elasticity force limit, the soft tissue of the seed and grain is not crushed. Equation of seed motion is written within the working limit of the equipment on the basis of force impact of certain limit. As the diameter of the rolling hub is wider, seed is more grasped and held between working gaps according to the research conclusion. When friction coefficiency between compressing deck and seeds surface is higher, seeds make action and motion between working surfaces. It is necessary to determine speed change between working gaps in determining creativity of the peeling equipment and power of the electric motor. Therefore, using energy saving law, we determined seed speed to be exited from seed peeling equipment by concerning equation.

Keywords: the peeling equipment, rolling hub, compressing deck, elasticity deformation, peeling seed, period changing force, friction coefficiency, working gap, elasticity coefficiency.

References

[1] The essential course of theoretical mechanics by N.N. Nikitin, 1990s.
[2] Agricultural and miller equipment. Elements of the theory of working processes, calculation of adjustment parameters and operating modes. N.I.Klenin. V.A. Sakun. 1980.
[3] Experimental results of determining the limit of elastic deformation of buckwheat depending on its moisture content. O. Amartuvshin. 2021.
[4] Theoretical estimation of the speed of the motion of the processed materials in the tangential threshing device of seed. Aleshkin. A. V, Simonov. MV, Mokiev. V. Yu. Technique and technology, APK. 2018.

Microstructure, phase transformation and mechanical properties of Ni-Ti-Hf-La alloys

Munkhjargal Badamdorj[1], Dovchinvanchig Maashaa[2]

[1,2]*School of Applied Sciences, Mongolian University of Life Sciences, Ulaanbaatar, 17024, Mongolia*

Email: dovchinvanchig@muls.edu.mn

Ni-Ti shape memory alloy materials have unique characteristics such as superelasticity and non-corrosion. Ni-Ti-Hf alloy is considered as candidates for high-temperature applications. However, no studies have been conducted on the La addition to NiTiHf alloy. Therefore, the influence of La addition on the structure, the phase transformation, and the mechanical properties of NiTiHf alloys remains unclear.

The effects of rare earth element La addition on the microstructure, phase transformation and mechanical properties of $Ni_{50}Ti_{30}Hf_{20-x}La_x$ (x =0, 0.5, 1 and 2) alloys were investigated experimentally. The results showed that the microstructure of Ni-Ti-Hf-La quaternary alloys consists of the Ni-Ti-Hf matrix and La precipitates. One-step phase transformation was observed in all Ni-Ti-Hf-La quaternary alloys. The martensitic transformation starts temperatures decrease gradually with the increase of La content in Ni-Ti-Hf-La alloys. Increasing the La content can significantly improve the hardness and elastic modulus decreases gradually with of Ni-Ti-Hf-La alloys.

Keywords: Ni-Ti-Hf alloy, microstructure, martensitic transformation, hardness, elastic modulus

Effect of La addition Microstructure and Mechanical Property of Ti-Nb-La alloys

Bolormaa Dorjsuren, Dovchinvanchig Maashaa

School of Applied Sciences, Mongolian University of Life Sciences, Ulaanbaatar, 17024, Mongolia

Email: dovchinvanchig@muls.edu.mn

Ti-Nb based alloys have a shape memory effects (SMA) and elasticity behavior and have been used in various fields, particularly in engineering and industrial applications [1]. Current research interest on SMAs mainly lies in controlling the phase transformation temperature and improving the shape memory effect for their applications. The effects mechanical properties, microstructure and shape memory effect have been widely studied by adding transitional elements to Ti-Nb binary alloys. These elements include Fe [2], B [3], Pd [4], Pt [5], Zr[6], Al [7], Si [8], etc. It has been confirmed that an appropriate amount of rare-earth element La can affect the microstructure and phase transformation Ni-Ti-La alloys. However, little information about the addition of the rare earth element La to Ti-Nb alloys is reported up to now.

In this work, the effects of rare earth element La addition on the microstructure and mechanical properties of $Ti_{80}Nb_{20-x}La_x$ (x =0, 1 and 2) alloys were investigated experimentally. The results showed that the microstructure of Ti-Nb-La ternary alloys consists of the Ti-Nb matrix and La-rich precipitates. Increasing the La content can significantly improve the hardness and elastic modulus decreases gradually with of Ti-Nb-La alloys.

Keywords: Ti-Nb-La alloy, microstructure, hardness, elastic modulus

References

[1] Jani J M, Leary M, Subic A, et al. 2014. A Review of Shape Memory Alloy Research, Applications and Opportunities. Materials and Design. 56: 1078-1113.

[2] Ehtemam-Haghighi S, Liu Y, Cao G, et al. 2016. Phase Transition, Microstructural Evolution and Mechanical Properties of Ti-Nb-Fe Alloys Induced by Fe Addition. Materials and Design. 97: 279-286.

[3] Al-Zain Y, Kim HY, Miyazaki S. 2015. Effect of B Addition on the Microstructure and Superelastic Properties of a Ti-26Nb Alloy. Materials Science & Engineering A. 644: 85-89.

[4] Wu SQ, Ping DH, Yamabe-Mitarai Y. 2013. Microstructural Characterization

on Martensitic Phase in Ti-Nb-Pd Alloys. Journal of Alloys and Compounds. 577:423-426.

[5] Kim HY, Oshika N, Kim JI, et al. 2007 Martensitic Transformation and Superelasticity of Ti-Nb-Pt Alloys. Materials Transactions. 48(3): 400-406.

[6] Zhou Y, Li Y, Yang X, et al. 2009. Influence of Zr Content on Phase Transformation, Microstructure and Mechanical Properties of Ti75-xNb25Zrx(x=0-6) Alloys. Journal of Alloys and Compounds. 486: 628-632.

[7] Farooq MU, Khalid FA, Zaigham H, et al. 2014. Superelastic Behaviour of Ti-Nb-Al Ternary Shape Memory Alloys for Biomedical Applications. Materials Letters. 121: 58-61.

[8] Kim HS, Kim WY, Lim SH. 2006. Microstructure and Elastic Modulus of Ti-Nb-Si Ternary Alloys for Biomedical Applications. Scripta Materialia. 54: 887-891.

Characterization of Geological Materials from the Baganuur coal mine area

Sarantsetseg Purevsuren[1], Davaabal Batmunkh[2], Bayarzul Uyat[2], Narandalai Byamba-Ochir[1], Nyamdelger Shirchinnamjil[2], Oyun-Erdene Gendenjamts[2], Enkhtuul Surenjav[1*]

[1]Laboratory of Inorganic Chemistry, Institute of Chemistry and Chemical Technology, Mongolian Academy of Sciences, Ulaanbaatar 13330, Mongolia
[2]Laboratory of Material Science and Technology, Institute of Chemistry and Chemical Technology, Mongolian Academy of Sciences, Ulaanbaatar 13330, Mongolia

Email: enkhtuul@mas.ac.mn

Mongolia is rich in natural resources, with abundant mineral deposits including copper, iron, gold, uranium, rare earth elements, coal, phosphorite, and fluorspar. However, large quantities of mining waste are generated, and many of these resources remain underutilized. One such waste material is coal-series kaolin.

In this study, geological materials from the Baganuur coal mine, the largest coal mine in Mongolia, were characterized for their mineralogical composition. Samples were collected from five drill holes and two waste dumpsites, and analyzed using X-ray diffraction (XRD), X-ray fluorescence (XRF), thermogravimetric analysis (TG/DTA), and chemical analysis. XRD analysis revealed that the clay mineral samples contained quartz, kaolinite, muscovite, albite, illite, and clinochlore. XRF analysis showed the presence of major oxides including silica, aluminum, iron, magnesium, and titanium. Lithological characterization of drill holes A02, A03, A07, A08, and A10 was successfully completed. The aluminum oxide content reached a maximum of 19%, indicating a relatively low kaolinite content, far from the desired purity. Further purification of the clay samples is required to achieve a kaolinite content greater than 80%. The goal is to develop a high-performance kaolin-based mineral materials for various application through efficient separation and removal of kaolin from associated minerals and organic matter.

Keywords: mineralogical characterization, geological materials, coal-series kaolin, kaolinite

Liquid phase exfoliation of MoS_2 in aqueous IPA

O.Erdenetuya[1,a], B.Odontuya[1,b], Yu.Ganchimeg[1,c], E. Gurbadam[2,d], S.Jargalan[2,e], D.Otgonbayar[1,f], G. Batdemberel[1,g], D. Jamiyanaa[3,h], J.Battogtokh[4,i] and G. Munkhsaikhan[1,j*]

[1]*Department of Physics, School of Applied Sciences, Mongolian University of Science and Technology, Ulaanbaatar, Mongolia*
[2]*Center for Technology Minerals and Innovation, School of Geology and Mining Engineering, Mongolian University of Science and Technology, Ulaanbaatar, Mongolia*
[3]*Science Department, Chatham University, Pittsburgh, Pennsylvania, USA*
[4]*Jacobs Engineering Group, Hanover, Maryland, USA*

Email: gmunkhsaikhan@must.edu.mn

In this work, the liquid phase exfoliation (LPE) method was investigated to produce a large quantity of 2D MoS_2. The introduction of ultrasound into IPA and IPA/DI solutions containing MoS_2 resulted in fragmentation and exfoliation of the MoS_2. The determination of the layers of LPE-MoS_2 was performed by optical microscopy, atomic force microscopy and resonant Raman spectroscopy. Flakes with four to many layers were detected by AFM and resonant Raman investigations.

Keywords: 2D materials, ultrasonication, exfoliation, solvent.

Recovering possibilities of REEs from spent NiMH in Mongolia using hydrometallurgical methods

Togtokh Nergui[1], Ikhbayar Batsukh[1], Sarantuya Lkhagvajav[1], Munkhbaatar Adiya[1], Sevjidsuren Galsan[1]

[1]*Institute of Physics and Technology, Mongolian Academy of Sciences*

Email: togtokhn@mas.ac.mn

The promotion of the application of electrical vehicles (EV) and hybrid electrical vehicles (HEV) resulted in an enormous amount of waste NiMH battery waste all over the globe. Many countries are facing severe problems related to recycling technology of hazardous and environmentally harmful spent NiMH batteries. One of the most significant examples of this situation is Mongolia importing around 80% of total HEV vehicles from Japan. Unfortunately, Mongolia does not have a factory purpose for recycling the spent NiMH batteries. Therefore, our study investigated the recovering possibilities of rare earth elements (REE) in the anode material of NiMH batteries used in HEVs in Mongolia. However, REEs were fabricated as metal alloys with numerous metal contents including Ni, La, Nd, Pr, Co, and Fe which makes recovering the technology of REEs more challenging. To address this major problem, our study revealed the potential recovery of REEs in the anode material of spent NiMH batteries. The spent NiMH battery of a used Prius HEV was dismantled manually and then dissolved in 2 different acid media, namely, hydrochloric acid (HCl) and sulfuric acid (H_2SO_4) to produce corresponding metal salt solutions. Obtained metal salt solutions were characterized by elemental analysis through atomic absorption spectroscopy (AAS) and elemental contents were determined. Elemental analysis showed that nickel was the highest composition of anode material of spent NiMH battery with 6942 mg, also, lanthanum possess percentage with 2372 mg. Notably, other REEs were also detected such as Nd, Ce and Pr which confirms the presence valuable metal contents. Even more, crystallized metal salts showed Ni and La chloride peaks in X-ray diffraction (XRD) patterns confirming the presence of REEs in the anode material of spent NiMH batteries. Then, the metal salt solution undergoes 2 different processes: solvent extraction method using an organic extractor for obtaining complex compound containing REEs and precipitation method to produce insoluble double metal REE salts in the aqueous solution. As a result, the precipitation method showed promising results for recovering phase pure double metal salts containing REEs and a high recovering rate compared to the solvent extraction method. XRD patterns revealed that double metal salts consist of a variety of REE sulfates

including $NaLa(SO_4)_2$, $NaNd(SO_4)_2$, and $NaPr(SO_4)_2$ indicating there is great potential for reusing anode materials of spent NiMH as valuable REEs source for the global market.

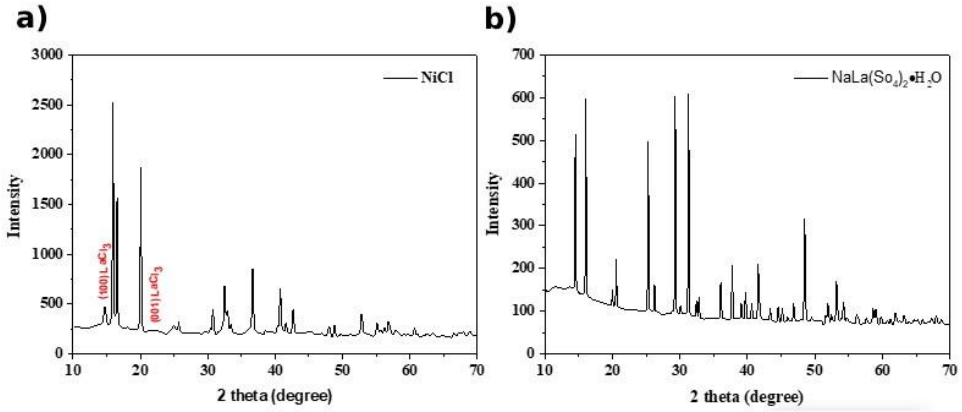

Figure 1. (a) X-ray diffraction (XRD) pattern results for crystalized salts obtained from the anode material from a NiMH battery dissolved by hydrochloric acid (b) X-ray diffraction (XRD) pattern of rare earth metal sulfates precipitated from the NiMH battery anode material by dissolved in H_2SO_4.

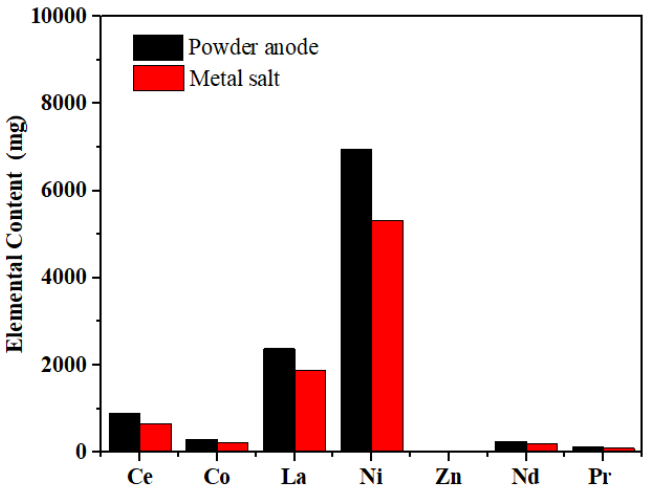

Figure 2. Determined elemental compositions for anode material of spent NiMH by using AAS.

References

[1] Holmberg, F., 2017. Recycling of Nickel Metal Hydride (NiMH) Batteries; Characterization and Recovery of Nickel, AB5 Alloy and Cobalt (Doctoral dissertation, Chalmers Tekniska Hogskola (Sweden)).

[2] Bertuol, D. A., Bernardes, A. M., & Tenório, J. A. S. (2009). Spent NiMH batteries—The role of selective precipitation in recovering valuable metals. Journal of Power Sources, 193(2), 914–923. https://doi.org/10.1016/j.jpowsour.2009.05.014

[3] Ahn, N.-K., Swain, B., Shim, H.-W., & Kim, D.-W. (2019). Recovery of Rare Earth Oxide from Waste NiMH Batteries by Simple Wet Chemical Valorization Process. Metals, 9(11), 1151. https://doi.org/10.3390/met9111151

[4] Azeroual, Hanae, et al. "NaLa (SO4) 2, H2O thermal conversion and Na3La (SO4) 3 crystal growth." Journal of Solid State Chemistry 317 (2023): 123570. https://doi.org/10.1016/j.jssc.2022.123570

Possible Application of Ni Microparticles Recovered from Spent NiMH Batteries for Water Splitting and Green Energy Technologies

Ikhbayar Batsukh[1], Togtokh Nergui[1], Sarantuya Lkhagvajav[1], Munkhbaatar Adiya[1], Sevjidsuren Galsan[1]

[1]*Institute of Physics and Technology, Mongolian Academy of Science*

Email: Ikhbayar_b@mas.ac.mn

In the last 2 decades, Mongolia became one of the biggest markets for second-hand hybrid electrical vehicles (HEV) mainly exported from Japan [1]. Therefore, this tight situation forces Mongolia to take urgent action to reduce and recycle the enormous amount of spent NiMH batteries in landfills and car repair centers. At the same time, so-called waste NiMH batteries reached their end-of-life state and contain a high amount of metals including Ni and rare earth elements (REEs) [2]. These metals are crucial raw materials for all electrochemical cells such as batteries, supercapacitors, and electrochemical catalysts sustaining green energy. More specifically, Nickel is widely known for its high electrochemical activity, affordability, and natural abundance. Unfortunately, mining nickel directly from natural ores requires a high amount of energy and produces tons of CO_2 emissions in nature making the exploitation of nickel an environmentally harsh option [3]. Thus, recycling and recovering nickel and other metals from spent NiMH batteries accumulated in Mongolia could solve the global shortage of nickel and also contribute to the advancement of sustainable green energy technologies. To achieve this goal, our current study suggests that Ni microparticles synthesized from leachate achieved from the cathode material of spent NiMH batteries show promising electrochemical activity toward water splitting. Ni microparticles exhibited exponential increase beyond and before the Faradaic reaction range indicating oxygen evolution reaction (OER) and hydrogen evolution reaction (HER) reaction takes place on the surface of Ni microparticles. To understand electrocatalytic activity and the mechanism of Ni microparticles, linear sweep voltammetry, and Tafel plots were obtained via electrochemical characterization techniques. Ni microparticles attached to the surface of a glassy carbon electrode (GCE) are used as an electrochemical catalyst and showed overpotential values of 338 mV and 157 mV for OER and HER respectively. The overpotentials obtained for Ni microparticles were relatively closer to RuO_2 conventional noble metal catalysts for electrochemical water splitting technologies [4,5]. The Tafel slopes of Ni microparticles for electrochemical water splitting were found to be 199

mV/dec-1 and 197 mV/dec-1 which was higher than RuO_2. This is mainly due to the larger particle size resulting in increased charge-transfer resistance (R_{ct}) value making the catalyst consist of Ni microparticles requiring higher potential to further increase the current density. Even though, our results suggest that Ni microparticles synthesized from $NiCl_2$ solution recovered from spent NiMH battery can be competing candidates for electrochemical water splitting technologies. This proves that recycling the spent NiMH for electrochemical catalysts can convert toxic battery waste into economic and environmental profit.

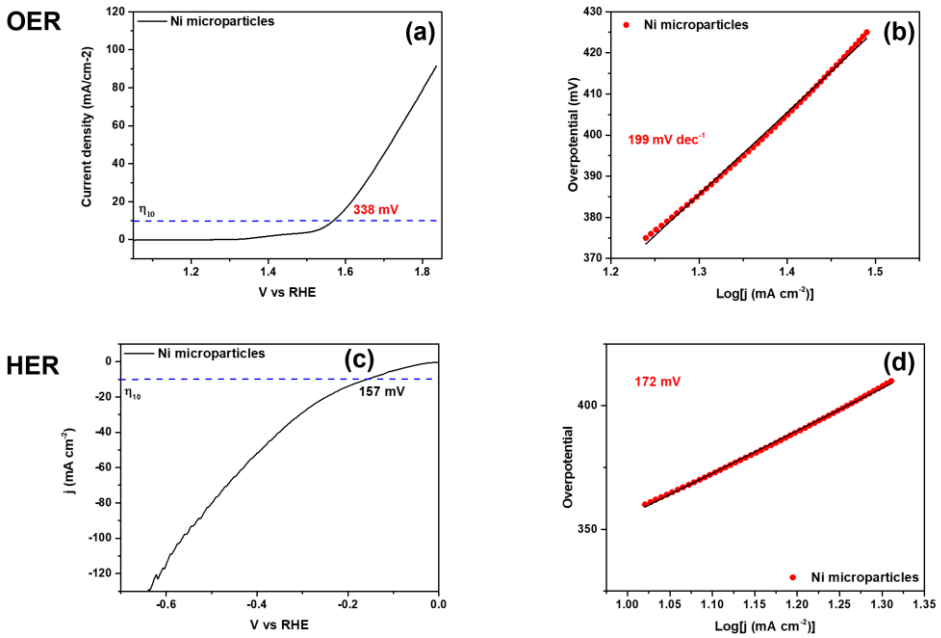

Fig. 1. (a) LSV curves of Ni microparticles for OER, (b) Tafel plot for OER, (c) LSV curves of Ni microparticles for HER, (d) Tafel plot for HER.

References

[1] S. Wang, J. Yu, K. Okubo, Scenario Analysis on the Generation of End-of-Life Hybrid Vehicle in Developing Countries—Focusing on the Exported Secondhand Hybrid Vehicle from Japan to Mongolia, Recycling 4 (2019) 41. https://doi.org/10.3390/recycling4040041.

[2] K. Larsson, C. Ekberg, A. Ødegaard-Jensen, Dissolution and characterization of HEV NiMH batteries, Waste Management 33 (2013) 689–698. https://doi.org/https://doi.org/10.1016/j.wasman.2012.06.001.

[3] G.M. Mudd, Global trends and environmental issues in nickel mining: Sulfides versus laterites, Ore Geol Rev 38 (2010) 9–26. https://doi.org/https://doi.org/10.1016/j.oregeorev.2010.05.003.

[4] Y. Qin, T. Yu, S. Deng, X.-Y. Zhou, D. Lin, Q. Zhang, Z. Jin, D. Zhang, Y.-B.

He, H.-J. Qiu, L. He, F. Kang, K. Li, T.-Y. Zhang, RuO2 electronic structure and lattice strain dual engineering for enhanced acidic oxygen evolution reaction performance, Nat Commun 13 (2022) 3784. https://doi.org/10.1038/s41467-022-31468-0.

[5] N. Cong, Y. Han, L. Tan, C. Zhai, H. Chen, J. Han, H. Fang, X. Zhou, Y. Zhu, Z. Ren, Nanoporous RuO2 characterized by RuO(OH)2 surface phase as an efficient bifunctional catalyst for overall water splitting in alkaline solution, Journal of Electroanalytical Chemistry 881 (2021) 114955. https://doi.org/https://doi.org/10.1016/j.jelechem.2020.114955.

Obtaining carbon nanoparticles by pulse laser influence in a double-pulse mode in an aquatic environment

Anisovich A.G.[1], M.I.Markevich[2], V.I. Zhuravleva[3], Zh.Vanchinhuu[4], Sainsanaa Tserenchimed[4]

[1]*Institute of Applied Physics of the National Academy of Sciences of Belarus*
[2]*Physical-Technical Institute of the National Academy of Sciences of Belarus*
[3]*Military Academy of the Republic of Belarus*
[4]*Department of Physics, Mongolian State University,*

Email: anna-anisovich@yandex.ru

A synthesis was carried out and the surface morphology of carbon nanoparticles obtained in the process of laser ablation of a carbon target was studied. The synthesis was carried out in an aqueous environment using radiation from a yttrium aluminum garnet laser (LS-2134D) with a wavelength of 1064 nm. A two-pulse laser mode was used. The pulses were separated by a time interval of 3 μs. The pulse duration was 10 ns, the pulse repetition rate was 10 Hz, and the energy of a single pulse was 0.05 J. It has been shown that during laser ablation a set of nanoparticles of various sizes and shapes is formed. The possibility of controlling the process of ablation and synthesis of carbon nanoparticles has been demonstrated. Efficient generation of nanoparticles for use in various applications has been achieved.

Keywords: nanoparticles, laser irradiation, nanosecond pulse duration, double-pulse mode, carbon

Fluorophosphate glass for fluorescence thermometry: optimization of holmium and ytterbium ions concentration

A. S. Piotukh[1], E.V. Kolobkova[2], V.A. Orlovich[1], I. A. Khodasevich[1]

[1]B.I.Stepanov Institute of Physics NAS of Belarus, Minsk, Belarus
[2]Saint-Petersburg state institute of technology, Technical University, St. Petersburg, Russia

Email: i.khodasevich@dragon.bas-net.by

The report contains the results of research on determination of the thermal stability for fluorophosphate glasses doped by rare earth ions Yb^{3+} and Ho^{3+} using the fluorescence intensity ratio (FIR) method. These glasses are attractive due to low phonon losses and intensive upconversion fluorescence (UCF). The aim of the work was to study the influence of temperature on UCF of Ho^{3+} ions and to find the optimal concentration of rare earth ions suitable for thermometry applications. UCF spectra were measured in the temperature range from + 25 °C to + 200 °C for different powers of CW diode laser generating the radiation in the 950-965 nm range.

The FIR dependences were calculated from the recorded UCF spectra in the green and red regions. It turned out, that the ratios of the intensities of the sub-bands near the wavelengths of 543 nm / 657 nm, as well as the wavelength ranges within the bands of green and red fluorescence, were more sensitive to temperature changes. The linearity of the dependences increased with an growth in the radiation power of the diode laser from 0.4 to 1 W.

Optimization of the concentration of Yb^{3+} ions in glasses with a constant content of Ho^{3+} ions (0.1 mol %) shows that the glass with 5 mol % Yb^{3+} has relative thermal sensitivity (S_r) of 0.38 % K^{-1} (298 K) and the best calibration line. The glass sample with 0.5 mol % Ho^{3+} and 5 mol % Yb^{3+} ions, excited by the diode laser power of 0.4 W, exhibits the maximum S_r of 0.49 % K^{-1} at 298 K and the best calibration line. Additionally, it achieves a temperature resolution (δT) of ± 0.5 K. The results obtained are exceed in S_r fluoroborate glasses [1], are comparable with the parameters of $KLu(WO_4)_2$ nanocrystals [2] and TZBYH3 glass [3] and exceed these materials in δT. The FIR dependences selected are well approximated by a linear function with a correlation coefficient close to 1. So, they can be used for calibration of the sensor elements of the temperature detectors.

Thus, the method of measuring spectra that we have developed allowed us to select glasses with high values of relative thermal sensitivity, the FIR dependences of which are acceptable as calibration lines for sensor

elements of temperature sensors.

The authors acknowledge the partial financial support of the researches from the State Program for scientific investigations “Photonics and microelectronics for innovations” (task 1.2).

References

[1] Limin Liu, Junhao Xing, Fei Shang, Guohua Chen, Structure and up-conversion luminescence of Yb^{3+}/Ho^{3+} co-doped fluoroborate glasses, Optics Communications, Volume 490, 2021, 126944, ISSN 0030-4018

[2] Ho,Yb:$KLu(WO_4)_2$ Nanoparticles: A Versatile Material for Multiple Thermal Sensing Purposes by Luminescent Thermometry / O. A. Savchuk, J. J. Carvajal, M. C. Pujol, E. W. Barrera, J. Massons, M. Aguilo, F. Diaz // J. Phys. Chem. C. 2015, 119, 32, 18546–18558

[3] V. Lojpur, M. Nikolic, L. Mancic, O. Milosevic, M.D. Dramicanin, Y_2O_3:Yb,Tm and Y_2O_3:Yb,Ho powders for low-temperature thermometry based on up-conversion fluorescence / Ceram. Int. Volume 39, Issue 2, 2013, Pages 1129-1134

SRS in compressed hydrogen by two-pulse biharmonic pump: modeling and experiment

R.V. Chulkov[1], J. Davaasambuu[2], G. Shilagardi[2], L.E. Batay[1], A.S. Grabtchikov[1], A.I. Vodchits[1], V.A. Orlovich[1]

[1]Institute of physics of NAS of Belarus, Pr. Nezavisimosti 68-2, Minsk, Belarus
e-mail: v.orlovich@dragon.bas-net.by
[2]Laser Research Center of the National University of Mongolia, Ulan-Bator, Mongolia

A model has been created describing the generation of stimulated Raman scattering (SRS) in the field of biharmonic pumping. The effects of diffraction, wave detuning and non-collinear propagation of exciting radiation beams are taken into account. Based on the model, modeling the characteristics of the SRS converted radiation has been performed for the specific experimental conditions – SRS generation in compressed hydrogen at excitation by the radiation beams of nanosecond neodymium laser at the wavelengths of 1064 nm (the main, fundamental harmonic) and 532 nm (the second harmonic).

It is shown that when pumping by the second harmonic radiation (hydrogen pressure is 12 atm, the length of the hydrogen cell is 120 cm, the focal length of the lens focusing the pump radiation is 100 cm, the pulse duration of the exciting radiation is 10 ns), the excitation threshold of SRS is reached at an energy of laser pulses of 20 mJ. At pumping the hydrogen by the fundamental harmonic radiation, the SRS generation threshold increases to about 100 mJ and above. Biharmonic multi-frequency pumping, when the SRS gain increment at the second harmonic wavelength reaches a value of ≥ 9, makes it possible to reduce the threshold of SRS excitation by the radiation of the fundamental harmonic by about 10 times. The reason of this is explained by the fact that the radiation of the main harmonic is parametrically (threshold-free) scattered on a dynamic nonlinear lattice created by the powerful radiation of the second harmonic. The proposed method can be used for low-threshold SRS generation of the radiation tunable in a wide frequency range of the infrared spectral range.

An experimental setup has been created to study the SRS process under conditions of two-frequency two-pulse pumping. The setup uses a pulsed ($\approx$ 15 ns) Nd:YAG laser, which allows simultaneous generation on the main and second harmonics with the pulse energy up to 150 mJ and 100 mJ, respectively. Under conditions of single-pulse pumping by the radiation of the second harmonic, the SRS excitation threshold was $\leq$ 20 mJ. When the threshold was exceeded by about 4 times, the efficiency of

SRS conversion to the first Stokes component reached 13 %. With single-pulse pumping by the radiation of the fundamental harmonic, the SRS threshold was not reached at laser pulse energies of 100 mJ and more. The simultaneous use of the pulses of both harmonics made it possible to excite the SRS with the main harmonic at an energy of its pulses less than 20 mJ and obtain the generation at a wavelength of 1907 nm. The experimental data obtained are in good agreement with the calculation results.

The research was carried out within the framework of a joint Belarusian-Mongolian project funded by the Belarusian Republican Foundation for Fundamental Research (F23MN-008) and the Mongolian Foundation for Science and Technology.

Dielectric properties of liquid crystals in porous media

Chimytov Timur[1,2], Kalashnikov Sergey[1], Nomoev Andrey[1,2]

[1] *Institute of Physical Materials Science SB RAS*
Russia, 670047, Ulan-Ude, st .Sakhyanova, 6
[2] *Buryat State University named after Dorzhi Banzarov*
Russia, 670000, Ulan-Ude, st. Smolina, 24a

Email: tchimytov@gmail.com

Nematic liquid crystals (LC) in micron-sized pores embedded in polymer matrices suggest a new perspective on topologically different metastable states. These systems combine a number of practically useful properties such as the possibility of LC control by the external field, mechanical strength of the polymer. In addition, it has been observed that some of these systems exhibit an electromechanical memory effect, where the light transmission coefficient does not return to its original value after removal of the electric field. This means the orientational order in the system is partially fixed and memorized. In the early 1990s, by investigating LC dispersed in polymer structures with different morphologies, Yaamaguchi and coworkers showed that isolated pores do not induce significant memory effects [1-2]. In contrast, these effects are observed when the pores form a multi-connected structure in which the alignment of LC is permanently distorted. The memory effect can be used in a wide range of practical applications from the design of data storage systems to sensors in gas and liquid flow visualization systems.

The memory effect is characterized by the presence of hysteresis in the measurements of the capacity of LC cells. For our tasks, a specialized bridge impedance meter was designed and manufactured, which allows high-resolution measurements of the capacitance of LC cells with simultaneous application of a control voltage up to 120 V.

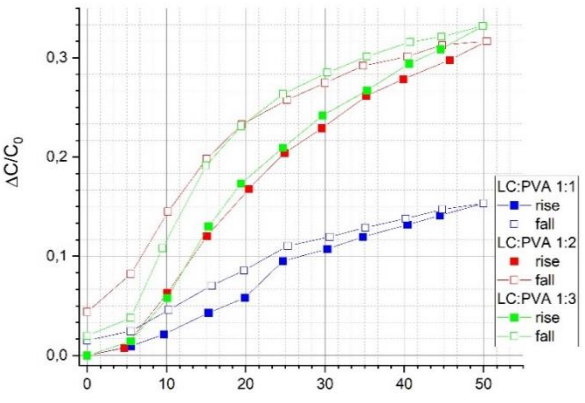

Figure 1

Figure 1 shows the dependence of the normalized the LC cells capacitance on the applied bias voltage. All investigated LC cells contain polymer-dispersed liquid crystal (PDLC) films consisting of a polymer (polyvinyl acetate - PVA) with dispersed nematic LC (5CB) in

different proportions: LC:PVA = 1:1, 1:2 and 1:3. Each concentration in the figure has a different color, with filled squares denoting measurements with increasing voltage and empty squares denoting measurements with decreasing voltage. At all concentrations hysteresis is clearly observed and capacitance of all samples does not return to the initial value, indicating the presence of the memory effect. However, the memory effect is maximal at the ratio of LC to PVA 1:2.

Figure 2 shows microscopy of PDLC films at different concentrations. The light areas correspond to PVA polymer and the dark areas to LC. In the polymer area, an unconnected porous structure with droplets size of about 5 μm is observed (figure 3). Thus, at a concentration of 1:1 LC is preferentially dispersed in such micropores and the memory effect is minimized in this case, which is consistent with Yamaguchi's result. When the LC:PVA ratio increases, interconnected LC structures of tens of microns in size are observed and the memory effect becomes significant. Finally, at a ratio 1:3 a large number of "snowflakes", which are topological defects in LC with +1 charge, are observed in these interconnected structures. Defects with this charge are point defects and seem to be responsible for the reduction of the memory effect.

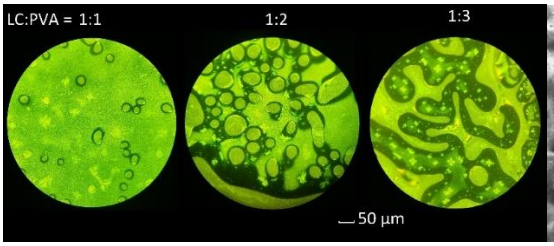

Figure 2

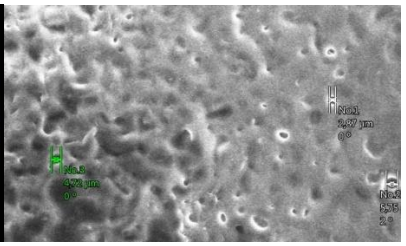

Figure 2

One of the possible mechanisms for suppressing the effect is related to the ability of defects to absorb part of the free electric charges of the LC and reduce the total capacitance.

References

[1] Yamaguchi, R., Sato S., Memory effects of light transmission properties in Polymer-Dispersed-Liquid-Crystal (PDLC) films // J. J Appl. Phys. 1991. Vol. 30, № 4A, P. L616.

[2] Yamaguchi R., Sato S., Highly transparent memory states in polymer d ispersed liquid crystal films // Liq. Cryst. 1993. Vol. 14, № 4. P. 929-935.

Optical Characterization of *Rosa baitagensis* Leaves Cultured In Vitro

Davaadulam G.[1,2], Begzsuren T.[1,2], Usukhjargal.D[3], Badamkhatan T.[1]

[1]*Laboratory of Radiation Biophysics, Institute of Physics and Technology, MAS*
[2]*Department of Physics, School of Arts and Sciences, NUM*
[3]*Laboratory of Plant Stress Physiology, Institute of Botanic Garden and Research, MAS*

Accurate estimation of foliar pigment content is essential for improving agricultural management, as it provides valuable information on plant health, disease detection, stress levels, and biochemical composition. Spectroscopic methods, particularly in the visible and infrared light ranges, allow for the reliable assessment of these factors through spectral data analysis. In this study, we measured the optical properties of *Rosa baitagensis* leaves cultured *in vitro* using a hyperspectral Liquid Crystal Tunable Filter (LCTF) camera. Hyperspectral analysis, which combines optical spectroscopy and image analysis, enabled the simultaneous evaluation of both physiological and morphological parameters. Image data were processed to extract the spectral signatures of the leaves, and a custom algorithm was developed to estimate foliar pigment content based on reflectance spectra. The results demonstrated that this algorithm can accurately quantify pigment content in Rosa baitagensis leaves, based on hyperspectral data captured by the LCTF.

Keywords: Hyperspectral camera, LCTF, reflectance, algorithm, *in vitro*

Effect of deposition on heat transfer enhancement using nanofluids on microscopic mechanism by molecular dynamics

Gantumur Tsend[1], Chen Qicheng[1]

[1] *School of energy and power enjineering, Northeast electric power university, China*

In this study, the heat transfer phenomenon of nanofluids in the box with 84.5 x 350 x 31.5 Å was studied by molecular dynamics simulation. It was shown that the interaction effect of Cu atoms, H_2O molecules, and MgO nano-particles on a smooth flat metal surface is caused by temperature. Simulation were performed using the Lennard-Jones liquid model, in which a monolith of magnesium oxide was boiled with water on a flat metal surface at temperatures from 700 to 3000 K. At temperatures of 800 K, 900 K, and 1200 K, water molecules were observed to follow MgO moves down to form a molecular cluster. Moreover, at 2700 K and 3000 K, most of the boiling of water molecules caused a sparse distribution, and some groups of metallic copper molecules were attracted to the increasing MgO and merged. These results indicate that the nanofluid heat transfer phenomenon occurs faster when MgO is bonded to the copper surface at low temperature.

Approximate temperature fields in two-layer cylinder at pulse thermal loading

P.L.Abiduev[1], T.G.Darmaev [2]

[1]*Buryat State University, Russia*
[2] *Buryat State University, Russia*

Email: dtumen@mail.ru

This paper discusses the temperature fields in the walls of hollow vessels of cylindrical shapes, inside which detonation of gas mixtures is carried out, accompanied by a powerful thermal shock with a very high gradient over time. In such chambers [1], for example, parts can be treated with heat stroke. Classical solutions to thermal conduction problems are obtained, as a rule, in the form of a sum of poorly converging series according to the eigenfunctions of the problem. They are very inconvenient for practical application on a short time interval due to the slow convergence of the series representing the solution. This inconvenience is especially pronounced when determining the maximum temperature values that are realized over a short time interval under the impulse effect of heat flow on the surface. As is known, temperature stresses pose the greatest danger to the strength of such thick-walled vessels.

The purpose of this work is to determine the approximate temperature field at small time values convenient for practical use. To do this, after transition to the Laplace plane of the images, the images decompose into a fast-converging series, holding the first term in the decomposition. Moving further to the plane of the original, we get a temperature field at small time values. For the case of a single-layer cylinder, it was possible to obtain simple analytical expressions. In general, numerical inversion of the obtained images is applied. For this, an effective modification of the numerical method for finding the original, proposed by A. Populis, is used. The modification increases the accuracy of calculations and improves the convergence of the resulting series. To determine the temperature field at small time values, a series of seven terms is obtained.

Approximate expressions are obtained for temperature fields with a sufficiently high degree of accuracy, suitable for small time values, where the highest temperatures occur. Comparisons were made with solutions for temperature fields obtained by the classical method.

References

[1] Plankovsky S.I., Gaidachuk A.V., Shipul O.V., Palazyuk E.S. Modeling of the process of melting burrs during thermal pulse treatment with detonating mixtures, Aerospace technology and technology, No. 3 (100). PP. 24-28 (2013).

Preparation and characterization of new porous carbon material from cow manure using pyrolysis

G. Narkhajid[1], S. Baasanjargal[1], S. Enkhtur[2], D. Rentsenmyadag[1], Ts. Ninjbadgar[3], G. Erdene-Ochir[2], S. Munkhtsetseg[2]

[1]Department of Chemistry, School of Arts and Sciences, National University of Mongolia
[2]Department of Physics, School of Arts and Sciences, National University of Mongolia
[3]Center for Nanoscience and Nanotechnology, National University of Mongolia

The development of environmentally friendly methods to process and utilize animal-derived biomass, particularly animal manure, has become increasingly important in Mongolia. Since the cattle population is reached more than sixty million heads in the pasture farming, the land faces animal waste issues in its everyday life more constantly.

Efforts to recycle animal biomass waste into valuable materials are already underway. Lignocellulosic and non-lignocellulosic biomass can be converted into biofuels through thermochemical processes such as torrefaction, pyrolysis, combustion, and gasification. High-quality biomass with a high density can be produced through thermal and chemical conversion processes.

In this work, we successfully obtained a new porous carbon material derived from cow manure. Cellulose was extracted from pure manure and then treated via the pyrolysis process. The resulting material was studied using elemental analysis, proximate analysis, thermogravimetric analysis (TGA), Fourier-transform infrared spectroscopy (FTIR), and electron paramagnetic resonance spectroscopy (EPR).

Research on the chemical composition and biological activity of Artemisia scoparia Waldst. et Kit.

M.Uyanga[1], B.Buyankhishig[2], D.Rentsenmyadag[1], T.Murata[3], J.Batkhuu[2]

[1]*Department of Chemistry, School of Arts and Sciences, National University of Mongolia*
[2]*Department of Chemical and Biological Engineering, School of Engineering and Technology, NUM*
Bioorganic Chemistry and Pharmacognosy Laboratory
[3]*Tohoku Medical and Pharmaceutical University*

Email: m.uyanga2004@gmail.com, d_rentsenmyadag@num.edu.mn

Isorhamnetin-3-O-β-D-glucoside was isolated and characterized from different seasonal variations of *Artemisia scoparia* and its bioactive properties were evaluated using DPPH radical scavenging assay. *Artemisia scoparia* was chosen for this research due to its significant ecological role in Mongolia's harsh environments, its seasonal biochemical variations, and its traditional medicinal uses, which suggest a potential for discovering bioactive compounds with health benefits. An extract was obtained by extracting the plant's summer sample three times using 80% acetone, resulting in a total yield of 20.8 g of pure extract. From this, 6 mg of the bioactive fraction SCO-6E was isolated through HPLC purification as a yellowish-white solid. The structure of the SCO-6E fraction was confirmed using Nuclear Magnetic Resonance (NMR) spectroscopy, identifying it as isorhamnetin-3-O-β-D-glucoside, a flavonoid with notable antioxidant, anti-inflammatory, and anticancer properties. The antioxidant activity of *Artemisia scoparia* was evaluated using the DPPH radical scavenging assay, revealing the highest activity in winter (IC_{50} = 93), moderate activity in summer (IC_{50} = 143), and the lowest activity in spring (IC_{50} = 243). These seasonal variations indicate that the plant’s bioactive compounds fluctuate with environmental conditions, enhancing its antioxidant potential during colder months. In conclusion, this research highlights the significance of seasonal variations in the bioactive compounds of *Artemisia scoparia*, suggesting that its extracts could serve as a valuable source of natural antioxidants and therapeutic agents. Further studies are warranted to explore its full potential in both agricultural and medicinal applications.

A Proposal of Mach-Zehnder Interferometer

S.A. Nomoev[1], I.S. Vasilevskii[1]

[1]*National Research Nuclear University MEPhI (Moscow Engineering Physics Institute), Moscow, Kashirskoe highway 31, 115409, Russian Federation*

Email: serganom@gmail.com

The Mach-Zehnder Interferometer (MZI) based on silicon is a fundamental component in silicon photonic integrated circuits, garnering significant interest for its applications in optical modulators, optical switching, and optical routing. This work delves into the exploration of various MZI structures.

The MZI serves as a device employed to assess the relative variations in phase shift between two beams originating from a single source. Leveraging the MZI concept, various optical modulators have been suggested for photonic-electronic integration, including electro-optic modulators and more. This work introduces a MZI and provides simulation results to elucidate its functionality.

We simulate the MZI using Lumerical INTERCONNECT and obtain the spectrum of the interferometer. We choose the TE mode in this simulation, and the path length difference is 100 μm. In fig. 1, transmission spectrum of the MZI with 220×500-nm^2 waveguide cross-section is plotted for three different path lengths (ΔL=25, 103.054 and 149.274 μm), for the fundamental quasi-TE. It can be interpreted that the larger the path length difference, the more the peaks in the spectrum and the smaller the Free Spectral Range (FSR). The pink line ΔL=25, the blue line ΔL=103.054 and the green line ΔL=149.274 μm.

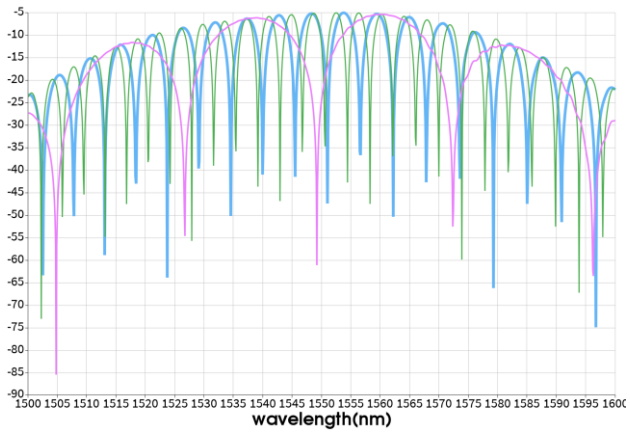

Fig. 1. Transmission spectrum of the MZI with cross-section of 500×220 nm^2 for three different path lengths (ΔL= 25, 103.054 and 149.274 μm)

The layout of devices was designed with Klayout, and the GDS file was sent for fabrication. The devices were fabricated using 100 keV Electron Beam Lithography [1]. The fabrication used silicon-on-insulator wafer with 220 nm thick silicon on 3 μm thick silicon dioxide. The substrates were 25 mm squares diced from 150 mm wafers.

To characterize the devices, a custom-built automated test setup [2] with automated control software written in Python was used [3].

We propose several Mach-Zehnder interferometers with different ΔL using silicon strip waveguide. The simulation results coincide with our experimental results.

References

[1] R. J. Bojko, J. Li, L. He, T. Baehr-Jones, M. Hochberg, and Y. Aida, Electron beam lithography writing strategies for low loss, high confinement silicon optical waveguides, *J. Vacuum Sci. Technol.*, B 29, 06F309 (2011).

[2] Lukas Chrostowski, Michael Hochberg, chapter 12 in "Silicon Photonics Design: From Devices to Systems", Cambridge University Press, 2015

[3] http://siepic.ubc.ca/probestation, using Python code developed by Michael Caverley.

Spectral methods in the study of metal-fullerene films

E. M. Shpilevsky[1], O.G. Penyazkov[1], S., A. Filatov[1], G. Shilagardi[2], D. Ulam-Orgikh[2], S. Munkhtsetseg[2]

[1]*A.V. Luikov Heat-Mass Transfer Institute, NAS of Belarus, Minsk*
[2]*National University of Mongolia, Ulaanbaatar, Mongolia*

Email: espilevsky@rambler.ru, fil@hmti.ac.by

In the presented work the features of formation of metal-fullerene films of the systems Al-C_{60}, Au-C_{60}, Cu-C_{60}, Ti-C_{60} from atomic-molecular flows in vacuum were investigated, the processes of surface resonance plasmon absorption and diffusion were studied. It is shown that electron microscopy, optical, Auger-electron and X-ray spectroscopy methods are effective for the study of metal-fullerene films.
The combination of different methods of spectroscopy and electron microscopy allowed to establish the dependence of the grain size of the films, the shift of the position of the plasmon absorption maximum, diffusion parameters on the ratio of metal and fullerene components, to establish the fact of formation of the chemical compound Cu_6C_{60}.

Keywords: fullerene, metal-fullerene films, electron microscopy, optical, electron and X-ray spectroscopy methods, structure, physical properties.

Fine powders and advanced materials

S.P. Bardakhanov

Khristianovich Institute of Theoretical and Applied Mechanics of SB RAS, 630090, Novosibirsk, Russia

The aim of our research is the creation of prototypes of products utilizing the newest electronic component base and to introduce into circulation the latest technology of inorganic nanoparticles; those with a relatively simple morphology, a composite core-shell, Janus-like in character, stellate, and wire-rod nanoobjects. For the first time in Russia, and in the world, such nanoparticles were obtained by the author and colleagues between 2004 and 2011 using a new original and high-performance technology of gas-phase synthesis.

The results of these studies into the corresponding effects in semiconductor and composite metal-insulator, metal-semiconductor nanoobjects were published jointly with Mongolian colleagues between 2007 and 2011 and has become widely known on both Russian and international scientific literature. The projects and work were jointly funded by the Russian Foundation for Basic Research, the Russian and Mongolian Academies of Sciences, and the Mongolian National University.

Organised chronologically, and starting in 2001, significantly "nonequilibrium" formations were obtained in the form of silicon nanoparticles coated with a thin (2 nm) layer of oxide, highly defective silver nanoparticles coated with specific silver oxide particles with sizes of several nm, and Cu@Si core- shell composite particles: $SiO:SiO_2$, $Ag@Si:SiO:SiO_2$, Janus-like Ta&Si ($TaSi_2$&Si), Cu&Zn and $SiC\&Si:SiO_2$ nanoparticles of various morphologies.

Special attention is paid to morphologically non-trivial semiconductor substances in nanoform, a number of which were obtained in earlier work. New unique properties have already been discovered in relation to the effects of photoluminescence, photovoltaics, photoconductivity, Raman scattering. The intension is to optimize them for energy conversion in electro-optics and deepening the analysis of quantum and nonlinear effects when exciting nanoobjects, of various morphologies, with powerful LEDs of the near, medium, and deep ultraviolet light range, and laser radiation.

New types of nanoparticles are also tested, containing other metals (Ni, Co, Mo, W, Hf, Nb, Au, Os, Bi, etc.) and in semiconductor combinations (Si, Ge, Sn, in combination with their oxides, and a number of other oxides, for example, Cu_2O, which the authors had obtained earlier). This will lead to a comprehensive study of the crystallographic, electrical,

optical and magnetic properties of the corresponding prototypes using concepts arising from modern spintronics and magnonics.

Corresponding efforts are pursued in the direction of carbides as well as other compounds. The team have already obtained SiC, WC, W_2C, W_3C, YC_2, AlC_3 and others, nitrides AlN, TiN, SiN, and already studied approaches to the nanomodification of A_3B_5 compounds, in particular, gallium arsenide, indium. An important objective is to 'design' and demonstrate the possibility of creating prototypes of electronic 'devices' using as many as possible of different types of solitary particles obtained. For example, transistors, tiristors, diodes, photodiodes, phototransistors, photoresistors, LEDs, lasers, luminescent and thermoelectric elements and others.

The topic is of particular relevance for Russia, since its industrial circles have, for decades, needed to recognize the growing lag in the latest developments in the field of microminiaturization, and moreover, the virtual destruction of the electronic components industry. If the research is successful, there will be grounds not only to catch up with technologically more developed countries, but also to ensure a fundamentally advanced construction of industry on a completely new and revolutionary technological basis. The research exceeds the world level, and most of the experimental results were and will be obtained for the first time in the world.

This work was supported by a grant from the Russian Science Foundation under project No. 23-19-00258.

Determination of dielectric properties of liquid in nanoscale layer

Chingis Gulgenov*, Ivan Simakov, Sayana Bazarova and Ksenia Artem'eva

Institute of Physical Materials Science of the SB RAS, Ulan-Ude, 670047, Russia

*Email: chingisbarga@gmail.com

The real and imaginary parts of the dielectric permittivity of adsorbed water were determined by utilising the isotherms of surface acoustic wave (SAW) velocity changes during polymolecular adsorption. The adsorption of water vapour was conducted on the optically polished surface of the adsorbent, which was an acoustic line comprising a lithium niobate piezoelectric crystal in the *YZ*-cut configuration. The research tool employed was surface acoustic waves of the Rayleigh type, generated and recorded by SAW transducers within the frequency range of 20–400 MHz. The frequency dependencies of the real and imaginary parts of the complex dielectric permittivity of adsorbed water were investigated. For a range of thicknesses of the adsorbed layer within the investigated frequency range, a process of dielectric relaxation was observed. This phenomenon can be well interpreted by Debye's theory with a single relaxation time. The dielectric relaxation time of adsorbed water depends on the thickness of the adsorbed layer and significantly (by 2–3 orders) exceeds the relaxation time of water in the bulk liquid phase.

Elimination of Contradictions in the Phase Diagrams of Ternary Systems Sb-Sn-M (M=Ag,Bi,In,Ga,Zn) by the 3D Computer Models

Maria Parfenova[1], Vera Vorob'eva[1], Vasily Lutsyk1[, 2], Anna Zelenaya[1]

[1]*Institute of Physical Materials Science SB RAS*

[2]*Banzarov Buryat State University*

Email: vluts@ipms.bscnet.ru

The phase diagrams of ternary systems {Ag, Bi, In, Ga, Zn}-Sb-Sn are of significant importance for the development of lead-free solders and other electronic materials [1-2]. However, a significant discrepancy arises concerning the behavior of the incongruently melting binary compound Sb2Sn3. Some studies [3-4] suggest that Sb2Sn3 decomposes at 242.4°C into Sb and Sn, while other studies [5-7] indicate that it remains stable down to 300 K. This discrepancy hampers the establishment of a thermodynamically calculated phase diagram. In this study, we propose a novel approach to resolve these contradictions by employing 3D computer models. Our methodology involves the creation of a specialized scheme of phase states (not only phase reactions) in a 2D tabular form, which is subsequently transformed into a 3D format to construct a prototype of the phase diagram. These phase diagrams play a crucial role in understanding the phase relations and behavior of ternary alloys. By assembling a 3D model of the phase diagram prototype, the intricate geometric structure of the T-x-y diagram is visually and graphically explained, utilizing the scheme of mono- and nonvariant transformations. Real base points are incorporated, and the curvature of lines and surfaces is corrected to transform the prototype into a 3D model of the real T-x-y diagram [8]. The model enables the analysis of crystallization, microstructure formation, and the generation of material balances. We consider two versions of the scheme of mono- and invariant states for {Ag, Bi, In, Ga, Zn}-Sb-Sn systems, along with their corresponding 3D models. This comprehensive approach allows us to overcome the contradictions in the phase diagrams and provides valuable insights into the phase behavior of these ternary systems. The results of this study contribute to the advancement of lead-free solder materials and pave the way for further research in this field.

This work was been performed under the program of fundamental research SB RAS (project 0270-2021-0002).

References

[1] V.A. Lysenko, J. Alloys Compd., 776(5), 850-857 (2019).
[2] V.A. Lysenko, Russ. J. Phys. Chem. A., 94(9), 1747-1755 (2020). doi:10.1134/S0036024420090174.
[3] Atlas of Phase Diagrams for Lead-Free Soldering compiled by A. Dinsdale, A. Watson, A. Kroupa et al, COST 531. European Science Foundation, Brno, Czech Republic, 2008. V. 1. 289 pp.
[4] A. Kroupa, J. Vízdal, Defect and Diffusion Forum, 263, 99-104(2007).
[5] S.-W. Chen, P.-Y. Chen, C.-N. Chin et al, Metall. Mater. Trans. A., 39A, 3191-3198 (2008).
[6] W. Gierlotka, Y.-C. Huang, S.-W. Chen, Metall. Mater. Trans. A., 39A, 3199-3209 (2008).
[7] S.W. Chen, C.C. Chen, W. Gierlotka et al, J. Electron. Mater., 37(7), 992-1002 (2008).
[8] V.I. Lutsyk, V.P. Vorob'eva, A.E. Zelenaya, Acta Phys. Pol. A, 133(4), 763-766 (2018).